Exploring the Effects of Changping Decoction on Irritable Bowel Syndrome by Pathway and Pharmacology Network Bioinformatics Analysis

Guo-Jie Hu (huguojie2003@163.com)
The affiliated hospital of Qingdao University https://orcid.org/0000-0001-9844-8548
Ding Li
The Affiliated Hospital of Qingdao University
Shi-Fang Li
Department of Neurosurgery, The affiliated hospital of Qingdao University
Xiao-Yuan Li
Department of Traditional Chinese Medicine, The affiliated hospital of Qingdao University
Xiao-Wei Sun
Department of Traditional Chinese Medicine, The affiliated hospital of Qingdao University
Tian-Yue Sun
Basic medicine, Medical college, Qingdao University

Research

Keywords: Changping decoction, irritable bowel syndrome, pathway analysis, pharmacology, inflammation

Posted Date: November 18th, 2020

DOI: https://doi.org/10.21203/rs.3.rs-107301/v1

Abstract

Background An increasing body of research has confirmed the effectiveness of Traditional Chinese Medicine (TCM) for the treatment of irritable bowel syndrome (IBS).

Methods We explored the potential mechanism of *Changping* decoction (CPD) in the treatment of IBS through pathway analysis based on a network pharmacology approach. Public databases, including the Traditional Chinese Medicine Systems Pharmacology Database and Analysis Platform, Gene Expression Omnibus, and STRING, were used to screen the active ingredients and targets of CPD. Enrichment analysis was performed using the R-3.6.0 software to expound the biological functions and related pathways of CPD targets. The Cytoscape software was used to construct a “disease-CPD-target” network and identify hub genes of CPD relevant for the treatment of IBS. Employing rat models, pathological observation and abdominal withdrawal reflex tests were used to verify the effectiveness of CPD in the treatment of IBS. Immunohistochemistry was used to confirm the relationship between the CPD treatment and hub genes.

Results Network pharmacological analysis of CPD for the treatment of IBS identified 159 active ingredients. A total of 118 key targets were identified, including MAPK8, VEGFA, PTGS2, and others. A series of signaling pathways, such as MAPK, Kaposi sarcoma-associated herpesvirus infection, and IL-17 signaling pathway were found to play an important role in the therapeutic mechanism of CPD in the treatment of IBS. Pathological observation and abdominal withdrawal reflex tests confirmed that the symptoms of IBS in rats were relieved by CPD. Moreover, immunohistochemistry confirmed that CPD could inhibit the expression of inflammation-associated factors, such as VEGFA, MAPK8, and PTGS2.

Conclusions Based on network pharmacology analysis, the present study provides insights into the potential mechanism of CPD in the treatment of IBS after successfully screening for associated key target genes and signaling pathways. These findings establish a theoretical basis for the development of CPD-derived therapeutics.

Background

Irritable bowel syndrome (IBS) is one of the most commonly diagnosed conditions in primary care, accounting for approximately 10–20% of all clinical visits[1]. According to the current diagnostic standard for IBS, the Rome IV criteria, IBS is a chronic, relapsing, and remitting functional disorder of the gastrointestinal tract characterized by abdominal pain, bloating, and changes in bowel habits[2]. Because of a poor understanding of its pathophysiology, IBS is classified as a functional disorder whose diagnosis depends on the history of manifested symptoms [35, 36, 37]. The cause of IBS is unknown, and research in this area currently focuses on mucosal inflammation, genetic and immunological factors, alteration of the human microbiota, and alterations of intestinal permeability, as well as dietary and neuroendocrine factors, establishing that low-grade intestinal inflammation plays a key role in the pathophysiology of IBS[22, 23, 24, 25].

Despite considerable research efforts, the treatment of IBS remains a significant challenge mainly owing to its poorly defined pathophysiology. Traditional Chinese medicine (TCM) has provided various therapeutics for treating gastrointestinal disorders over centuries[5, 6]. An increasing body of evidence has revealed that natural medicinal active ingredients may have beneficial effects for the treatment of IBS, and these effects are likely to be multifactorial. Among host-related factors, intestinal inflammation, central alterations (i.e., aberrant stress responses and cognitive dysfunctions), peripheral alterations, intestinal mucosal barrier integrity, and intestinal flora, as well as neurotransmitters and hormones in the enteric nervous system (ENS), are believed to be involved[7, 27, 28, 29].

In this conceptual framework, herbs appear as an attractive option in terms of both efficacy and safety, while prebiotics, synbiotics, and antibiotics require further study[45]. A variety compounds found within herbs regulate complex targets, in turn modulating known and unknown mechanisms. Among herbal therapies, *Changping* decoction (CPD), which includes herbs widely used for treating gastrointestinal disorders, is a classic TCM prescription. The aim of this study was to provide evidence for the beneficial effects of CPD on IBS through pharmacology and pathway bioinformatics analyses, highlighting the relationship between immune-related pathways and IBS pathophysiology, which was further confirmed *in vivo*. Our study aimed to systematically explore the potential mechanism of CPD in the treatment of IBS and, thus, provides a theoretical basis for the development of CPD-derived therapeutics.

Methods

Target prediction of CPD ingredients

CPD is composed of baishao (Paeoniae Radix Alba), cangzhu (Atractylodes Lancea (Thunb. Dc)), chuanlianzi (Toosendan Fructus), dangshen (Codonopsis Radix), fuzi (Aconiti Lateralis Radix Praeparata), gancao (licorice), ganjiang (Zingiberis Rhizoma), huanglian (Coptidis Rhizoma), and huangqin (Scutellariae Radix). The Traditional Chinese Medicine Systems Pharmacology Database and Analysis Platform (TCMSP, https://www.tcmspw.com/tcmsp.php) is a comprehensive Chinese herbal medicine analysis tool that can be used to identify relationships between drugs, targets, and diseases based on 499 Chinese pharmacopoeia-registered herbs, as well as structural information for 29,384 ingredients[8,9,10]. In this study, the major compounds and related targets of CPD were screened from the TCMSP database. The screening criteria were oral bioavailability >30% and drug-like properties >0.15.

Prediction of IBS-related targets

The Gene Expression Omnibus (GEO, http://www.ncbi.nlm.nih.gov/geo/) is an international public repository for high-throughput microarray and next-generation sequencing functional genomic datasets[11]. In this study, we selected a dataset (GSE36701[12], GPL570) from the GEO database using the following keywords: “IBS” and “Homo sapiens.” The data of normal samples and IBS samples from GSE36701 were used for differential gene expression analysis by employing the Wilcoxon test from the

“limma” package in the R-3.6.0 software. The false discovery rate was set at <0.05, and an absolute value of log2 | fold change |> 1 was set as the cut-off value.

Screening the intersection of CPD targets and IBS targets

We screened the intersection of CPD targets and IBS targets through the VENNY2.1 online tool (https://bioinfogp.cnb.csic.es/tools/venny/index.html).

Construction a protein–protein interaction (PPI) network and screening of hub genes through which CPD regulates IBS

The drug–target interaction network was constructed using Cytoscape 3.7.2 software. The network had 129 nodes, including 9 drugs, 118 common target genes, 1 disease, and 1786 edges (Figure 2B). The STRING database (http://string-db.org) provides a critical assessment and integration of PPIs, including physical as well as functional associations[13]. The “CytoHubba” package in Cytoscape 3.7.2 software is a tool for exploring the core genes of the PPI network based on 11 calculation methods. MCC, a newly proposed method, has better performance with regard to precision of hub gene prediction from the PPI network[14,15]. In this study, we input the intersection of CPD targets and IBS targets in the STRING database to obtain a PPI network (Organism set to *Homo sapiens*) and then screened hub genes using the “CytoHubba” package.

Gene Ontology (GO) and Kyoto Encyclopedia of Genes and Genomes (KEGG) pathway enrichment analysis

The “clusterProfiler” package is an ontology-based R package that not only automates the process of biological term classification and the enrichment analysis of gene clusters but also provides a visualization module for displaying analysis results[16]. We used the “clusterProfiler” package in the R-3.6.0 software to perform enrichment analysis on the intersection of CPD targets and IBS targets to confirm the potential mechanism of CPD in the treatment of IBS. To determine the core mechanism of action of CPD in IBS, we analyzed the core 10 targets to determine the major signaling pathways by enrichment analysis.

Animals and treatment

Thirty-two SPF Wistar rats[17] weighing 220 (±20) g were provided by Pengyue Laboratory Animal Center, Jinan, Shandong, China (License: SCXK20190003). The rats were raised in the SPF animal room of the medical college, Qingdao University, Qingdao, Shandong, China (License: SYXK20150003). The rats were

isolated and fed for 1 week while they adapted to the environment and were then randomly divided again into a blank group (n = 8), model group (n = 8), CPD treatment group (n=8), and control treatment group (n = 8). According to the random number table method, 4 rats were fed in one cage for a total of 4 weeks. All rats had free access to drinking water and food. The room temperature was 24 (±2) °C, the relative humidity was 50 (±5)%, light and dark conditions were alternated every 12 h, and the rat cages were cleaned every 2 days. The model group, CPD treatment group, and control treatment group underwent water avoidance stress (WAS) for 1 h/day for 10 days[18,19]. Briefly, rats were weighed and placed on a platform (8 × 6 cm) affixed to the center of a plastic container (55 × 50 cm) which was filled with water to 1 cm below the platform. The conversion of the human dose to that used in rats was calculated based on body surface. The CPD treatment group was administered CPD for 14 consecutive days. CPD was prepared by mixing a solid aqueous extract in distilled water (1.125 mg/ml) and administered at a dose of 1.0 ml/220 g body weight. The control treatment group was given saline (1.0 ml/220 g) for 14 consecutive days.

Abdominal withdrawal reflex (AWR)

The AWR is mainly assessed to detect visceral hypersensitivity by dilating the rectum and colon to confirm whether the IBS model was successfully established[20,21]. In this study, all rats were fasted for 24 h but did receive drinking water. A small balloon dipped in liquid paraffin was then slowly inserted up to 4 cm into the colon. Subsequently, the rats received 10–80 mmHg pressure stimulation successively, each time increasing by 10 mmHg. The Al-Chaer method was used to evaluate the AWR score. When the abdominal wall of the rat is lifted from the bottom and contracted, or the rat body arches with elevation of the pelvis and scrotum, it is considered that the rat has a visceral pain threshold. The same pressure stimulations were performed three times, and the average pressure value was taken as the final score.

Histological observation and Immunohistochemistry

After the rats were sacrificed, colonic biopsies were obtained and fixed in cold 4% paraformaldehyde, embedded in paraffin, sectioned, stained with H&E, followed by gradient alcohol (100% twice, 95%, 70%, and 50% for 5 min each) and xylene dehydration (three times, for 5 min each). The colonic biopsy samples were observed under a light microscope (Olympus, Tokyo, Japan).

Immunohistochemistry experiments were performed on paraffin-embedded, 4-mm-thick sections. The sections were first incubated with the primary antibody at 37 °C for 60 min. The primary antibodies used were as follows: rabbit polyclonal anti-mouse VEGFA (1:100 dilution; Affinity Biosciences, Cincinnati, OH, USA), rabbit polyclonal anti-mouse MAPK8 (1:100; Affinity Biosciences), rabbit polyclonal anti-mouse PTGS2 (1:100; Affinity Biosciences). Thereafter, sections were incubated with a universal secondary antibody (1:200; Affinity) at 37 °C for 30 min and then visualized using diaminobenzidine (DAB). Finally, the nuclei were labeled by counterstaining the sections with hematoxylin. Three randomly selected fields

from each section were scanned under an Olympus CX31 microscope (Olympus, Tokyo, Japan), and quantitative analysis of immunohistochemistry results was performed using Image-pro plus software.

Statistical analysis

Graph Prism version 5.0 software was used to analyze the results. The statistical data are expressed as the mean ± standard deviation and were analyzed using the Wilcoxon rank-sum test.

Results

Results of CPD target protein and IBS disease target protein screening

A total of 159 active ingredients (Table 1) and 189 related target proteins were screened in the TCMSP database. Differential expression analysis identified a total of 13,634 differentially expressed genes, of which 6140 were downregulated, and 7494 were upregulated (Figure 1). According to the VENN diagram, a total of 118 target proteins were screened at the intersection of IBS and CPD (Figure 2A).

Table 1
Results of CPD target protein and IBS disease target protein screening

Molecular ID	Molecular name	OB(%)	DL
MOL001918	paeoniflorgenone	87.59	0.37
MOL001919	(3S,5R,8R,9R,10S,14S)-3,17-dihydroxy-4,4,8,10,14-pentamethyl-2,3,5,6,7,9-hexahydro-1H-cyclopenta[a]phenanthrene-15,16-dione	43.56	0.53
MOL001924	paeoniflorin	53.87	0.79
MOL000211	Mairin	55.38	0.78
MOL000358	beta-sitosterol	36.91	0.75
MOL000359	sitosterol	36.91	0.75
MOL000422	kaempferol	41.88	0.24
MOL000492	(+)-catechin	54.83	0.24
MOL000173	wogonin	30.68	0.23
MOL000184	NSC63551	39.25	0.76
MOL000188	3β-acetoxyatractylone	40.75	0.22
MOL000085	beta-daucosterol_qt	36.91	0.75
MOL001494	Mandenol	42	0.19
MOL001495	Ethyl linolenate	46.1	0.2
MOL002045	Stigmasterol	43.41	0.76
MOL002056	(E)-3-[(2S,3R)-2-(4-hydroxy-3-methoxy-phenyl)-7-methoxy-3-methylol-2,3-dihydrobenzofuran-5-yl]acrolein	54.74	0.4
MOL002058	40957-99-1	57.2	0.62
MOL000098	quercetin	46.43	0.28
MOL001006	poriferasta-7,22E-dien-3beta-ol	42.98	0.76
MOL002879	Diop	43.59	0.39
MOL003036	ZINC03978781	43.83	0.76
MOL000449	Stigmasterol	43.83	0.76
MOL003896	7-Methoxy-2-methyl isoflavone	42.56	0.2
MOL004355	Spinasterol	42.98	0.76
MOL005321	Frutinone A	65.9	0.34

MOL000006	luteolin	36.16	0.25
MOL006774	stigmast-7-enol	37.42	0.75
MOL007059	3-beta-Hydroxymethyllenetanshiquinone	32.16	0.41
MOL007514	methyl icosa-11,14-dienoate	39.67	0.23
MOL008393	7-(beta-Xylosyl)cephalomannine_qt	38.33	0.29
MOL008397	Daturilin	50.37	0.77
MOL008400	glycitein	50.48	0.24
MOL008407	(8S,9S,10R,13R,14S,17R)-17-[(E,2R,5S)-5-ethyl-6-methylhept-3-en-2-yl]-10,13-dimethyl-1,2,4,7,8,9,11,12,14,15,16,17-dodecahydrocyclopenta[a]phenanthren-3-one	45.4	0.76
MOL008411	11-Hydroxyrankinidine	40	0.66
MOL002211	11,14-eicosadienoic acid	39.9	0.2
MOL002388	Delphin_qt	57.76	0.28
MOL002392	Deltoin	46.69	0.37
MOL002395	Deoxyandrographolide	56.3	0.31
MOL002398	Karanjin	69.56	0.34
MOL001484	Inermine	75.18	0.54
MOL001792	DFV	32.76	0.18
MOL002311	Glycyrol	90.78	0.67
MOL000239	Jaranol	50.83	0.29
MOL002565	Medicarpin	49.22	0.34
MOL000354	isorhamnetin	49.6	0.31
MOL003656	Lupiwighteone	51.64	0.37
MOL000392	formononetin	69.67	0.21
MOL000417	Calycosin	47.75	0.24
MOL004328	naringenin	59.29	0.21
MOL004805	(2S)-2-[4-hydroxy-3-(3-methylbut-2-enyl)phenyl]-8,8-dimethyl-2,3-dihydropyrano[2,3-f]chromen-4-one	31.79	0.72
MOL004806	euchrenone	30.29	0.57
MOL004808	glyasperin B	65.22	0.44
MOL004810	glyasperin F	75.84	0.54

MOL004811	Glyasperin C	45.56	0.4
MOL004814	Isotrifoliol	31.94	0.42
MOL004815	(E)-1-(2,4-dihydroxyphenyl)-3-(2,2-dimethylchromen-6-yl)prop-2-en-1-one	39.62	0.35
MOL004820	kanzonols W	50.48	0.52
MOL004824	(2S)-6-(2,4-dihydroxyphenyl)-2-(2-hydroxypropan-2-yl)-4-methoxy-2,3-dihydrofuro[3,2-g]chromen-7-one	60.25	0.63
MOL004827	Semilicoisoflavone B	48.78	0.55
MOL004828	Glepidotin A	44.72	0.35
MOL004829	Glepidotin B	64.46	0.34
MOL004833	Phaseolinisoflavan	32.01	0.45
MOL004835	Glypallichalcone	61.6	0.19
MOL004838	8-(6-hydroxy-2-benzofuranyl)-2,2-dimethyl-5-chromenol	58.44	0.38
MOL004841	Licochalcone B	76.76	0.19
MOL004848	licochalcone G	49.25	0.32
MOL004849	3-(2,4-dihydroxyphenyl)-8-(1,1-dimethylprop-2-enyl)-7-hydroxy-5-methoxy-coumarin	59.62	0.43
MOL004855	Licoricone	63.58	0.32
MOL004856	Gancaonin A	51.08	0.43
MOL004857	Gancaonin B	48.79	0.47
MOL004863	3-(3,4-dihydroxyphenyl)-5,7-dihydroxy-8-(3-methylbut-2-enyl)chromone	66.37	0.41
MOL004864	5,7-dihydroxy-3-(4-methoxyphenyl)-8-(3-methylbut-2-enyl)chromone	30.49	0.41
MOL004866	2-(3,4-dihydroxyphenyl)-5,7-dihydroxy-6-(3-methylbut-2-enyl)chromone	44.15	0.41
MOL004879	Glycyrin	52.61	0.47
MOL004882	Licocoumarone	33.21	0.36
MOL004883	Licoisoflavone	41.61	0.42
MOL004884	Licoisoflavone B	38.93	0.55
MOL004885	licoisoflavanone	52.47	0.54
MOL004891	shinpterocarpin	80.3	0.68
MOL004898	(E)-3-[3,4-dihydroxy-5-(3-methylbut-2-enyl)phenyl]-1-(2,4-	46.27	0.31

	dihydroxyphenyl)prop-2-en-1-one		
MOL004903	liquiritin	65.69	0.74
MOL004904	licopyranocoumarin	80.36	0.65
MOL004907	Glyzaglabrin	61.07	0.35
MOL004908	Glabridin	53.25	0.47
MOL004910	Glabranin	52.9	0.31
MOL004911	Glabrene	46.27	0.44
MOL004912	Glabrone	52.51	0.5
MOL004913	1,3-dihydroxy-9-methoxy-6-benzofurano[3,2-c]chromenone	48.14	0.43
MOL004914	1,3-dihydroxy-8,9-dimethoxy-6-benzofurano[3,2-c]chromenone	62.9	0.53
MOL004915	Eurycarpin A	43.28	0.37
MOL004924	(-)-Medicocarpin	40.99	0.95
MOL004935	Sigmoidin-B	34.88	0.41
MOL004941	(2R)-7-hydroxy-2-(4-hydroxyphenyl)chroman-4-one	71.12	0.18
MOL004945	(2S)-7-hydroxy-2-(4-hydroxyphenyl)-8-(3-methylbut-2-enyl)chroman-4-one	36.57	0.32
MOL004948	Isoglycyrol	44.7	0.84
MOL004949	Isolicoflavonol	45.17	0.42
MOL004957	HMO	38.37	0.21
MOL004959	1-Methoxyphaseollidin	69.98	0.64
MOL004961	Quercetin der.	46.45	0.33
MOL004966	3'-Hydroxy-4'-O-Methylglabridin	43.71	0.57
MOL000497	licochalcone a	40.79	0.29
MOL004974	3'-Methoxyglabridin	46.16	0.57
MOL004978	2-[(3R)-8,8-dimethyl-3,4-dihydro-2H-pyrano[6,5-f]chromen-3-yl]-5-methoxyphenol	36.21	0.52
MOL004980	Inflacoumarin A	39.71	0.33
MOL004985	icos-5-enoic acid	30.7	0.2
MOL004988	Kanzonol F	32.47	0.89
MOL004989	6-prenylated eriodictyol	39.22	0.41

MOL004990	7,2',4'-trihydroxy□5-methoxy-3□arylcoumarin	83.71	0.27
MOL004991	7-Acetoxy-2-methylisoflavone	38.92	0.26
MOL004993	8-prenylated eriodictyol	53.79	0.4
MOL004996	gadelaidic acid	30.7	0.2
MOL000500	Vestitol	74.66	0.21
MOL005000	Gancaonin G	60.44	0.39
MOL005001	Gancaonin H	50.1	0.78
MOL005003	Licoagrocarpin	58.81	0.58
MOL005007	Glyasperins M	72.67	0.59
MOL005008	Glycyrrhiza flavonol A	41.28	0.6
MOL005012	Licoagroisoflavone	57.28	0.49
MOL005016	Odoratin	49.95	0.3
MOL005017	Phaseol	78.77	0.58
MOL005018	Xambioona	54.85	0.87
MOL005020	dehydroglyasperins C	53.82	0.37
MOL002464	1-Monolinolein	37.18	0.3
MOL002501	[(1S)-3-[(E)-but-2-enyl]-2-methyl-4-oxo-1-cyclopent-2-enyl] (1R,3R)-3-[(E)-3-methoxy-2-methyl-3-oxoprop-1-enyl]-2,2-dimethylcyclopropane-1-carboxylate	62.52	0.31
MOL002514	Sexangularetin	62.86	0.3
MOL001454	berberine	36.86	0.78
MOL002894	berberrubine	35.74	0.73
MOL002897	epiberberine	43.09	0.78
MOL002903	(R)-Canadine	55.37	0.77
MOL002904	Berlambine	36.68	0.82
MOL002907	Corchoroside A_qt	104.95	0.78
MOL000622	Magnograndiolide	63.71	0.19
MOL000785	palmatine	64.6	0.65
MOL001458	coptisine	30.67	0.86
MOL002668	Worenine	45.83	0.87

MOL001689	acacetin	34.97	0.24
MOL000228	(2R)-7-hydroxy-5-methoxy-2-phenylchroman-4-one	55.23	0.2
MOL002714	baicalein	33.52	0.21
MOL002909	5,7,2,5-tetrahydroxy-8,6-dimethoxyflavone	33.82	0.45
MOL002910	Carthamidin	41.15	0.24
MOL002913	Dihydrobaicalin_qt	40.04	0.21
MOL002914	Eriodyctiol (flavanone)	41.35	0.24
MOL002915	Salvigenin	49.07	0.33
MOL002917	5,2',6'-Trihydroxy-7,8-dimethoxyflavone	45.05	0.33
MOL002925	5,7,2',6'-Tetrahydroxyflavone	37.01	0.24
MOL002927	Skullcapflavone II	69.51	0.44
MOL002928	oroxylin a	41.37	0.23
MOL002932	Panicolin	76.26	0.29
MOL002933	5,7,4'-Trihydroxy-8-methoxyflavone	36.56	0.27
MOL002934	NEOBAICALEIN	104.34	0.44
MOL002937	DIHYDROOROXYLIN	66.06	0.23
MOL000525	Norwogonin	39.4	0.21
MOL000552	5,2'-Dihydroxy-6,7,8-trimethoxyflavone	31.71	0.35
MOL000073	ent-Epicatechin	48.96	0.24
MOL008206	Moslosooflavone	44.09	0.25
MOL010415	11,13-Eicosadienoic acid, methyl ester	39.28	0.23
MOL012245	5,7,4'-trihydroxy-6-methoxyflavanone	36.63	0.27
MOL012246	5,7,4'-trihydroxy-8-methoxyflavanone	72.24	0.26
MOL012266	rivularin	37.94	0.37

Construction the PPI network and hub gene screening

We constructed the PPI network from the STRING database, and a total of 120 nodes and 1354 edges were present in this network. According to the MMC calculation method, *MAPK8*, *VEGFA*, *MAPK1*, *CASP3*, *PTGS2*, *IL10*, *CXCL8*, *JUN*, *IL1B*, and *EGF* were recognized as core genes, playing major roles in the

mechanism of action of CPD in IBS. We believe that this PPI network can help us identify the potential mechanism of CPD in treating IBS (Figure 3).

Results of enrichment analysis

To explore the potential mechanism of CPD in the treatment of IBS, we performed GO enrichment analysis of the intersection of IBS and CPD using the R-3.6.0 software. For the biological process, terms such as response to nutrient levels (GO:0031667), response to extracellular stimulus (GO:0009991), and response to toxic substance (GO:0009636) were enriched (Figure 4A). For the cellular component, terms including membrane raft (GO:0045121), membrane microdomain (GO:0098857), and membrane region (GO:0098589) were enriched (Figure 4B). Protein heterodimerization activity (GO:0046982), chromatin binding (GO:0003682), and proximal promoter sequence-specific DNA binding (GO:0000987) were enriched for molecular function (Figure 4C). The results of KEGG analysis revealed that most targets were enriched in the AGE-RAGE signaling pathway in diabetic complications (hsa04933), Kaposi sarcoma-associated herpesvirus infection (hsa05167), and Hepatitis B (hsa05161) (Figure 5). Enrichment analysis of the core 10 proteins indicated that CPD mainly regulates pertussis (hsa05133), the IL-17 signaling pathway (hsa04657), the AGE-RAGE signaling pathway in diabetic complications (hsa04933), Kaposi sarcoma-associated herpesvirus infection (hsa05167), and the MAPK signaling pathway (hsa04010) (Figure 6A).

CPD alleviates intestinal visceral hypersensitivity in the WAS-induced IBS rat model

To determine whether CPD treatment could reduce intestinal visceral hypersensitivity in IBS, CPD was continuously administered via the intragastric route to IBS group rats for 2 weeks. The degree of colon pain threshold pressure was assessed by the AWR test. The colon pain threshold for the blank group and CPD treatment group was significantly lower than those for the model group and control treatment group ($P < 0.0001$) (Figure 7).

Results of histological observation and immunohistochemistry

Through histological observation, we found that the colon tissue of model group and control treatment group rats exhibited different degrees of lymphocyte proliferation, and no lesions were observed in colon tissues of the blank group and the CPD treatment group (Figure 8).

Immunohistochemistry analysis revealed that the expression of MAPK8, VEGFA, and PTGS2 in the model group and control treatment group samples was higher than that in the blank group and CPD treatment group (Figure 9).

Discussion

Identification of mechanisms that influence the efficacy of Chinese herbal formulae (CHF) for IBS might enable clinicians to predict the patient response and devise new more rational and tailored treatment strategies. In this study, to our knowledge for the first time, we report the anti-inflammatory effects of CPD mediated through the combined regulation of MAPK8, VEGFA, and PTGS2. The occurrence and development of IBS is a multilevel, multistep, complex process influenced by various factors, such as the gut microbiome, intestinal permeability, gut immune function, motility, diet, brain–gut interactions, and psychosocial status[2, 3, 4, 30]. This multitude of factors complicate the treatment of IBS. A recent study suggested some risk factors such as food allergy, abnormal microbiota, bile acid malabsorption, and increased intestinal permeability as contributors to low-grade intestinal inflammation, the major pathological manifestation in IBS.

Identification of important target proteins related to disease occurrence is essential for the exploration of IBS therapy-associated molecular mechanisms. Avoiding the restrictions of labor-intensive and time-consuming clinical trials with human subjects, *in silico* candidate target screening was employed. The target network consisted of 120 nodes and 1354 edges, and several topological parameters were calculated to obtain 10 important targets including hub or bottleneck proteins based on their high degree centrality and betweenness centrality. Pathway enrichment analysis yielded similar results. Overlapping targets, including PTGS2, VEGFA, MAPK8, CASP3, MAPK1, IL1B, EGF, JUN, IL10, and CXCL8, connected multiple subgroups, which may play pivotal roles in the pathway network [31, 32, 33, 34]. Importantly, several major targets were both hub bottleneck nodes in the structural network and key points in the protein and pathway networks. Based on gene function classification, our analysis results revealed that the efficacy of CPD therapy in IBS was based on the modulation of target proteins involved in the inflammatory response and oxidative stress regulation (MAPK8, PTGS2, VEGFA).

Histological observation revealed that the colons of model group and control treatment group rats exhibited low-grade inflammation characterized by lymphocyte proliferation, which was not observed in blank group and CPD treatment group rat colons. Increased numbers of lymphocytes have been reported in the colon and small intestine of patients with IBS. Our findings confirmed these observations in rats, and we further investigated the anti-inflammatory potential of CPD. A history of acute diarrheal illness preceding the onset of irritable bowel symptoms in some patients has suggested that the development of IBS occurs following infectious enteritis. The increased risk of post-infectious IBS is associated with bacterial, protozoan, helminth, and viral infections[41, 42, 43, 44, 45]. Some meta-analyses have shown an increased risk of IBS in patients who had experienced an episode of acute gastroenteritis[46,47]. A review of 18 studies showed a pooled 10% incidence of IBS and that the odds of developing IBS increased six-fold following acute gastrointestinal infection. One study in full-thickness jejunal biopsies supported our results, showing lymphocyte infiltration in the myenteric plexus as well as neuron degeneration, which stimulated the ENS, leading to abnormal motor and visceral responses within the intestine. Chronic infections have been suggested to trigger IBS symptoms in tandem with predisposing factors. Therefore, targeting the inflammatory pathways in IBS holds promise as an effective therapeutic approach.

The MAPK signaling pathway, to which MAPK8 belongs, is considered one of the classical inflammatory pathways [44]. Stool examinations from patients with diarrhea-predominant IBS have revealed a high level of serine-protease activity. The role of intestinal serine-proteases in the pathophysiology of IBS remains under investigation. In our study, we found that MAPK8 could regulate the expression of PTGS2 and VEGFA in Kaposi sarcoma-associated herpesvirus infection (hsa05167), thus, participating in the process of inflammation and cell proliferation (Fig. 6B) in IBS. MAPK8 could also regulate the expression of PTGS2 in the IL-17 signaling pathway (hsa04657) and, thus, participate in the process of autoimmune pathology, neutrophil recruitment, and immunity to extracellular pathogens (Fig. 6C). Further, immunohistochemistry demonstrated the potential of CPD to downregulate the expression of MAPK8 in an IBS rat model.

This notion is supported by the observation that CPD exerts its anti-inflammatory effects in colon tissue by inducing MAPK8 and PTGS2 in this experimental setup. PTGS2 was reported to play a critical role in regulating inflammatory responses by generating inflammatory mediator prostaglandin E-2 (PGE2) and contributed to the development of chronic inflammatory diseases [42, 43]. PGE2 plays an important role in the initiation of inflammation and pain. Mucosal PGE2 levels are increased in IBS, as reported in our study and in others. Prostaglandins are known to sensitize sensory neurons, including those innervating the gastrointestinal tract. PGE2, in turn, acts on DRG neurons to induce visceral hypersensitivity. There is little information regarding the use of COX2 inhibitors in patients with IBS. In a clinical study involving 61 patients with IBS-D diagnosed based on Rome IV criteria, 30-day treatment with mesalazine, a drug with anti-inflammatory properties, including cyclooxygenase and prostaglandin inhibition, effectively reduced key symptoms, such as stool frequency, abdominal pain, and bloating.

VEGFA is heavily involved in several chronic inflammatory disorders, where it not only promotes angiogenesis but also directly fosters inflammation [38, 39]. Angiogenesis is inherent to chronic inflammation and is associated with structural changes, including activation and proliferation of endothelial cells [40], as well as capillary and venule remodeling, all of which result in the expansion of the tissue microvascular bed. Studies have shown that the relationship between PTGS2 and VEGF is closely associated with inflammation and angiogenesis. It is now well established that, in diseases such as rheumatoid arthritis, psoriasis, atherosclerosis, and chronic lung inflammation, VEGFA is intimately involved in the pathogenesis, and targeting VEGFA is a promising new therapeutic strategy to dampen inflammation. In this study, we demonstrated activation of the VEGF pathway in actively inflamed IBD mucosa. The expression of both VEGFA and its receptor VEGFR-2 is enhanced in tissue biopsy specimens from inflamed bowel segments [41]. We next investigated whether CPD reduced the expression of VEGFA to exert its anti-inflammatory effects on intestinal endothelium *in vivo*. Our results identified VEGFA as intimately involved in IBD pathogenesis and at the crossroads between inflammation-driven angiogenesis and mucosal inflammation. This suggests that the CPD-mediated downregulation of VEGFA signaling may represent a new strategy to dampen intestinal inflammation.

We detected the expression of VEGFA, PTGS2, and MAPK8 in each group via immunohistochemistry, and found that CPD could effectively inhibit their expression. Further, low-grade inflammation in the colon tissue of rats and visceral pain were alleviated with CPD. Moreover, we showed that the increased PTGS activity and PTGS2 protein levels in HUVECs treated with VEGF were mediated through protein tyrosine kinases, but not protein kinase C (Figs. 4 and 5). These findings were consistent with those of previous studies showing that VEGF receptors on endothelial cells acted via protein tyrosine kinases, and the mitogen-driven induction of PTGS2 in endothelial cells was mediated through protein tyrosine kinases. Therefore, the downstream regulation of PG production in HUVECs activated with VEGF was affected at several points such as PTGS2, tyrosine phosphorylation, and phospholipase. In summary, our study is the first to show that PTGS2 can be induced through protein tyrosine kinase in HUVECs treated with VEGF. VEGF is known to be involved in pathological processes such as inflammation, atherosclerosis development, and carcinogenesis. Thus, the use of specific PTGS2 inhibitors in related conditions might have therapeutic potential.

Conclusion

Nowadays, a myriad of therapeutic options are available for IBS. However, treatment outcome remains unsatisfactory. Our research shows that CPD treatment can significantly alleviate intestinal visceral hypersensitivity and low-grade intestinal inflammation while also decreasing the expression of inflammation-related factors such as VEGFA and PTGS2 in IBS rats. These findings provide evidence that CPD can effectively relieve symptoms of IBS in patients. CPD is a traditional CHF including a number of medicinal plants with various therapeutic properties, traditionally used for different diseases including the treatment and prevention of intestinal disease. CHF contains different active agents and may act on multiple targets, signaling pathways, and biological processes with potential synergistic effects and chemical reactions. A total of 118 potential targets and 159 pharmacologically active components were identified for CPD, supporting the clinical potential of this TCM. As an increasing number of people tend to use TCM as alternative treatment, more extensive and well-designed preclinical and clinical trials assessing the potential synergistic and adverse side effects of herb–drug interactions, as well as mechanisms of action, will highlight future directions in IBS therapy research.

List Of Abbreviations

TCM – Traditional Chinese Medicine

CPD – *Changping* decoction
IBS – irritable bowel syndrome

GEO – Gene Expression Omnibus

PPI – protein–protein interaction

GO – Gene Ontology

KEGG – Kyoto Encyclopedia of Genes and Genomes

AWR – abdominal withdrawal reflex

CHF – Chinese herbal formulae

PGE2 – prostaglandin E-2

Declarations

Ethics approval

All applicable international, national, and institutional guidelines for the care and use of animals were followed. And all animal studies were approved by the Animal Ethics and Research Committee of The affiliated hospital of Qingdao University.

consent to participate

Not applicable.

Consent for publication

Not applicable

Availability of data and materials

Not applicable.

Competing interests

The authors declare that they have no competing interests.

Funding

This work was supported by grants from Natural Science Foundation

of China (82004128)

Authors’ contributions

GJH is responsible for the guarantor of integrity of the entire study, study concepts; DL and TYS are responsible for the experimental studies; SFL is responsible for the study design, experimental studies; XYL are responsible for the literature research; DL is responsible for the literature research, manuscript preparation & editing; XWS is responsible for the manuscript review. All authors read and approved the final manuscript.

Acknowledgements

Not applicable.

References

1. Sultan S, Malhotra A. Irritable Bowel Syndrome. Ann Intern Med. 2017;166(11):ITC81–96. doi:10.7326/AITC201706060.
2. Ford AC, Lacy BE, Talley NJ. Irritable Bowel Syndrome. N Engl J Med. 2017;376(26):2566–78. doi:10.1056/NEJMra1607547.
3. Chey WD, Kurlander J, Eswaran S. Irritable bowel syndrome: a clinical review. JAMA. 2015;313(9):949–58. doi:10.1001/jama.2015.0954.
4. Holtmann GJ, Ford AC, Talley NJ. Pathophysiology of irritable bowel syndrome. Lancet Gastroenterol Hepatol. 2016;1(2):133–46. doi:10.1016/S2468-1253(16)30023-1.
5. Rahimi R, Abdollahi M. Herbal medicines for the management of irritable bowel syndrome: a comprehensive review. World J Gastroenterol. 2012;18(7):589–600. doi:10.3748/wjg.v18.i7.589.
6. Liu JP, Yang M, Liu YX, Wei M, Grimsgaard S. Herbal medicines for treatment of irritable bowel syndrome. Cochrane Database Syst Rev. 2006;(1):CD004116. Published 2006 Jan 25. doi:10.1002/14651858.CD004116.pub2.
7. Xiao HT, Zhong L, Tsang SW, Lin ZS, Bian ZX. Traditional Chinese medicine formulas for irritable bowel syndrome: from ancient wisdoms to scientific understandings. Am J Chin Med. 2015;43(1):1–23. doi:10.1142/S0192415X15500019.
8. Ru J, Li P, Wang J, Zhou W, Li B, Huang C, Li P, et al. TCMSP: a database of systems pharmacology for drug discovery from herbal medicines. J Cheminform. 2014;6:13. Published 2014 Apr 16. doi:10.1186/1758-2946-6-13.
9. Wang P, Dai L, Zhou W, Meng J, Zhang M, Wu Y, Huo H, et al. Intermodule Coupling Analysis of Huang-Lian-Jie-Du Decoction on Stroke. Front Pharmacol. 2019;10:1288. doi:10.3389/fphar.2019.01288. Published 2019 Nov 5.
10. Yi F, Sun L, Xu LJ, Peng Y, Liu HB, He CN, Xiao PG. In silico Approach for Anti-Thrombosis Drug Discovery: P2Y1R Structure-Based TCMs Screening. Front Pharmacol. 2017;7:531. Published 2017 Jan 9. doi:10.3389/fphar.2016.00531.
11. Barrett T, Wilhite SE, Ledoux P, et al. NCBI GEO: archive for functional genomics data sets–update. Nucleic Acids Res. 2013;41(Database issue):D991–5. doi:10.1093/nar/gks1193.

12. Swan C, Duroudier NP, Campbell E, et al. Identifying and testing candidate genetic polymorphisms in the irritable bowel syndrome (IBS): association with TNFSF15 and TNFα. Gut. 2013;62(7):985–94. doi:10.1136/gutjnl-2011-301213.
13. Szklarczyk D, Franceschini A, Wyder S, et al. STRING v10: protein-protein interaction networks, integrated over the tree of life. Nucleic Acids Res. 2015;43(Database issue):D447–52. doi:10.1093/nar/gku1003.
14. Shannon P, Markiel A, Ozier O, et al. Cytoscape: a software environment for integrated models of biomolecular interaction networks. Genome Res. 2003;13(11):2498–2504. doi:10.1101/gr.1239303. PMID: 14597658.
15. Chin CH, Chen SH, Wu HH, Ho CW, Ko MT, Lin CY. cytoHubba: identifying hub objects and sub-networks from complex interactome. BMC Syst Biol. 2014;8(Suppl 4):11. doi:10.1186/1752-0509-8-S4-S11. Suppl 4) .
16. Yu G, Wang LG, Han Y, He QY. clusterProfiler: an R package for comparing biological themes among gene clusters. OMICS. 2012;16(5):284–7. doi:10.1089/omi.2011.0118.
17. O'Mahony SM, Bulmer DC, Coelho AM, et al. 5-HT(2B) receptors modulate visceral hypersensitivity in a stress-sensitive animal model of brain-gut axis dysfunction. Neurogastroenterol Motil. 2010;22(5):573-e124. doi:10.1111/j.1365-2982.2009.01432.x.
18. Vannucchi MG, Evangelista S. Experimental Models of Irritable Bowel Syndrome and the Role of the Enteric Neurotransmission. J Clin Med. 2018;7(1):4. Published 2018 Jan 3. doi:10.3390/jcm7010004.
19. Tran L, Chaloner A, Sawalha AH, Greenwood Van-Meerveld B. Importance of epigenetic mechanisms in visceral pain induced by chronic water avoidance stress. Psychoneuroendocrinology. 2013;38(6):898–906. doi:10.1016/j.psyneuen.2012.09.016.
20. Bai T, Li Y, Xia J, et al. Piezo2: A Candidate Biomarker for Visceral Hypersensitivity in Irritable Bowel Syndrome? J Neurogastroenterol Motil. 2017;23(3):453–63. doi:10.5056/jnm16114.
21. Mertz H, Naliboff B, Munakata J, Niazi N, Mayer EA. Altered rectal perception is a biological marker of patients with irritable bowel syndrome [published correction appears in Gastroenterology 1997 Sep;113(3):1054]. Gastroenterology. 1995;109(1):40–52. doi:10.1016/0016-5085(95)90267-8.
22. Chey WD. Food. The Main Course to Wellness and Illness in Patients With Irritable Bowel Syndrome. Am J Gastroenterol. 2016 Mar;111(3):366–71. doi:10.1038/ajg.2016.12. Epub 2016 Feb 9.
23. Ng QX, Soh AYS, Loke W, Lim DY, Yeo WS. The role of inflammation in irritable bowel syndrome (IBS). J Inflamm Res. 2018 Sep 21;11:345–349. doi: 10.2147/JIR.S174982.
24. Sánchez de Medina F, Romero-Calvo I, Mascaraque C, Martínez-Augustin O. Intestinal inflammation and mucosal barrier function. Inflamm Bowel Dis. 2014 Dec;20(12):2394–404. doi:10.1097/MIB.0000000000000204.
25. Spiller R, Major G. IBS and IBD - separate entities or on a spectrum? Nat Rev Gastroenterol Hepatol. 2016 Sep 26;13(10):613 – 21. doi: 10.1038/nrgastro.2016.141.

26. Li CY, Li SC. Treatment of irritable bowel syndrome in China: a review. World J Gastroenterol. 2015;21(8):2315–22. doi:10.3748/wjg.v21.i8.2315.
27. Chen Y, Xiao S, Gong Z, et al. Wuji Wan Formula Ameliorates Diarrhea and Disordered Colonic Motility in Post-inflammation Irritable Bowel Syndrome Rats by Modulating the Gut Microbiota. Front Microbiol. 2017;8:2307. doi:10.3389/fmicb.2017.02307. Published 2017 Nov 23.
28. Wang FY, Su M, Zheng YQ, et al. Herbal prescription Chang'an II repairs intestinal mucosal barrier in rats with post-inflammation irritable bowel syndrome. Acta Pharmacol Sin. 2015;36(6):708–15. doi:10.1038/aps.2014.170.
29. Li B, Rui J, Ding X, Chen Y, Yang X. Deciphering the multicomponent synergy mechanisms of SiNiSan prescription on irritable bowel syndrome using a bioinformatics/network topology based strategy. Phytomedicine. 2019;63:152982. doi:10.1016/j.phymed.2019.152982.
30. Grayson M. Irritable bowel syndrome. Nature. 2016;533(7603):101. doi:10.1038/533S101a.
31. Zhang GB, Li QY, Chen QL, Su SB. Network pharmacology: a new approach for chinese herbal medicine research. Evid Based Complement Alternat Med. 2013;2013:621423. doi:10.1155/2013/621423.
32. Hopkins AL. Network pharmacology: the next paradigm in drug discovery. Nat Chem Biol. 2008;4(11):682–90. doi:10.1038/nchembio.118.
33. Wu X, Jiang R, Zhang MQ, Li S. Network-based global inference of human disease genes. Mol Syst Biol. 2008;4:189. doi:10.1038/msb.2008.27.
34. Li S. Zhongguo. Zhong Yao Za Zhi. 2011;36(15):2017–20.
35. Sinagra E, Morreale GC, Mohammadian G, et al. New therapeutic perspectives in irritable bowel syndrome: Targeting low-grade inflammation, immuno-neuroendocrine axis, motility, secretion and beyond. World J Gastroenterol. 2017;23(36):6593–627. doi:10.3748/wjg.v23.i36.6593.
36. Barbara G, De Giorgio R, Stanghellini V, Cremon C, Corinaldesi R. A role for inflammation in irritable bowel syndrome? Gut. 2002;51(Suppl 1):i41–4. doi:10.1136/gut.51.suppl_1.i41. Suppl 1) .
37. Barbara G, Feinle-Bisset C, Ghoshal UC, et al. The Intestinal Microenvironment and Functional Gastrointestinal Disorders [published online ahead of print, 2016 Feb 18]. Gastroenterology. 2016;S0016-5085(16)00219–5. doi:10.1053/j.gastro.2016.02.028.
38. Zhang J, Huang Q, Zhao R, Ma Z. A network pharmacology study on the Tripteryguim wilfordii Hook for treatment of Crohn's disease. BMC Complement Med Ther. 2020;20(1):95. Published 2020 Mar 23. doi:10.1186/s12906-020-02885-9.
39. Scaldaferri F, Vetrano S, Sans M, et al. VEGF-A links angiogenesis and inflammation in inflammatory bowel disease pathogenesis. Gastroenterology. 2009;136(2):585 – 95.e5. doi:10.1053/j.gastro.2008.09.064.
40. Akarasereenont PC, Techatraisak K, Thaworn A, Chotewuttakorn S. The expression of COX-2 in VEGF-treated endothelial cells is mediated through protein tyrosine kinase. Mediators Inflamm. 2002;11(1):17–22. doi:10.1080/09629350210311.

41. Murphy JF, Fitzgerald DJ. Vascular endothelial cell growth factor (VEGF) induces cyclooxygenase (COX)-dependent proliferation of endothelial cells (EC) via the VEGF-2 receptor. FASEB J. 2001;15:1667–9. doi:10.1096/fj.00-0757fje.
42. Elshawi OE, Nabeel AI. Modulatory effect of a new benzopyran derivative via COX-2 blocking and down regulation of NF-κB against γ-radiation induced- intestinal inflammation. J Photochem Photobiol B. 2019;192:90–6. doi:10.1016/j.jphotobiol.2019.01.006.
43. Li Y, Soendergaard C, Bergenheim FH, et al. COX-2-PGE2 Signaling Impairs Intestinal Epithelial Regeneration and Associates with TNF Inhibitor Responsiveness in Ulcerative Colitis. EBioMedicine. 2018;36:497–507. doi:10.1016/j.ebiom.2018.08.040.
44. Yeung YT, Aziz F, Guerrero-Castilla A, Arguelles S. Signaling Pathways in Inflammation and Anti-inflammatory Therapies. Curr Pharm Des. 2018;24(14):1449–84. doi:10.2174/1381612824666180327165604.
45. Camilleri M. Management Options for Irritable Bowel Syndrome. Mayo Clin Proc. 2018 Dec;93(12):1858–1872. doi: 10.1016/j.mayocp.2018.04.032.

Figures

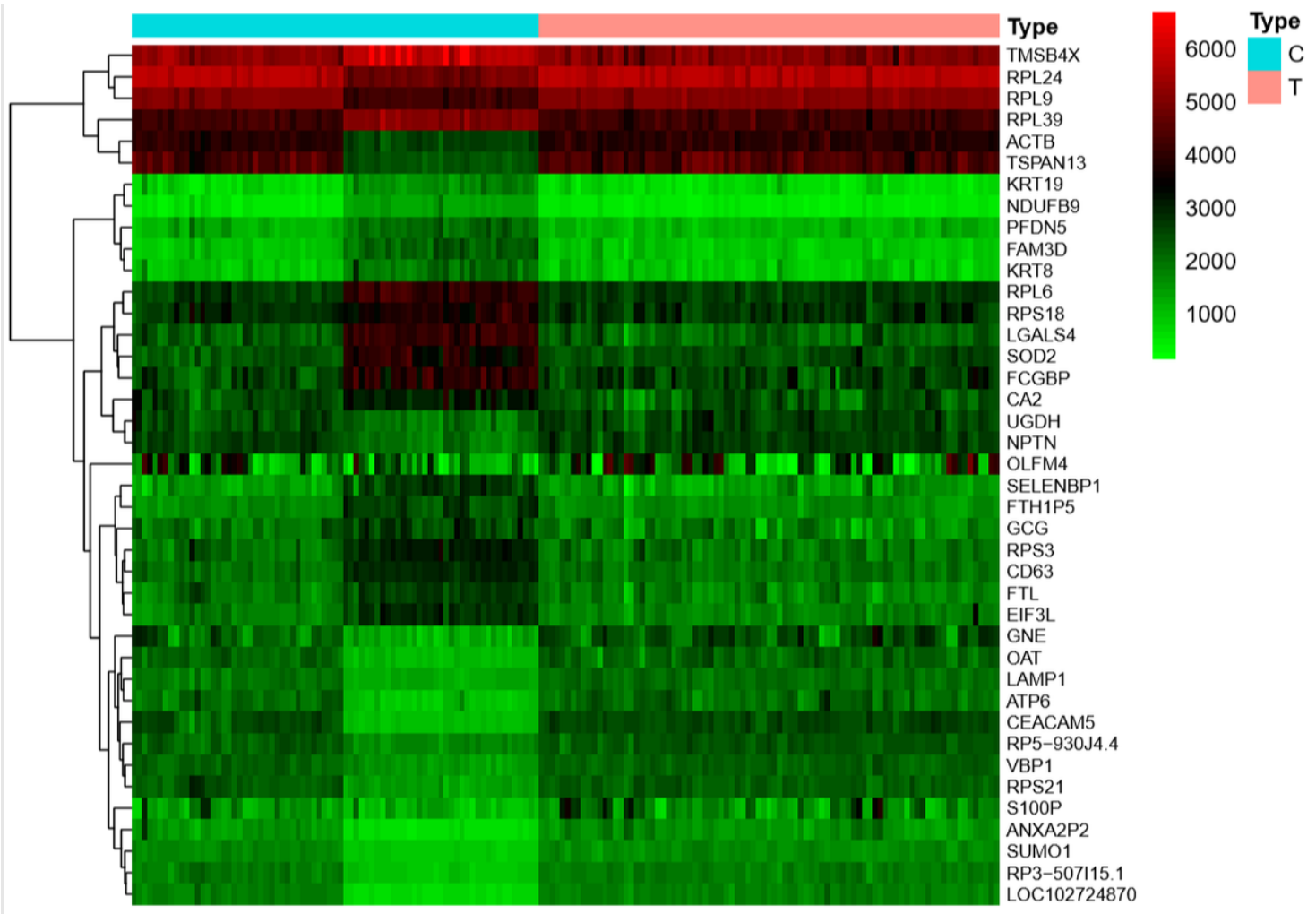

Figure 1

heatmap of difference analysis from GES36701

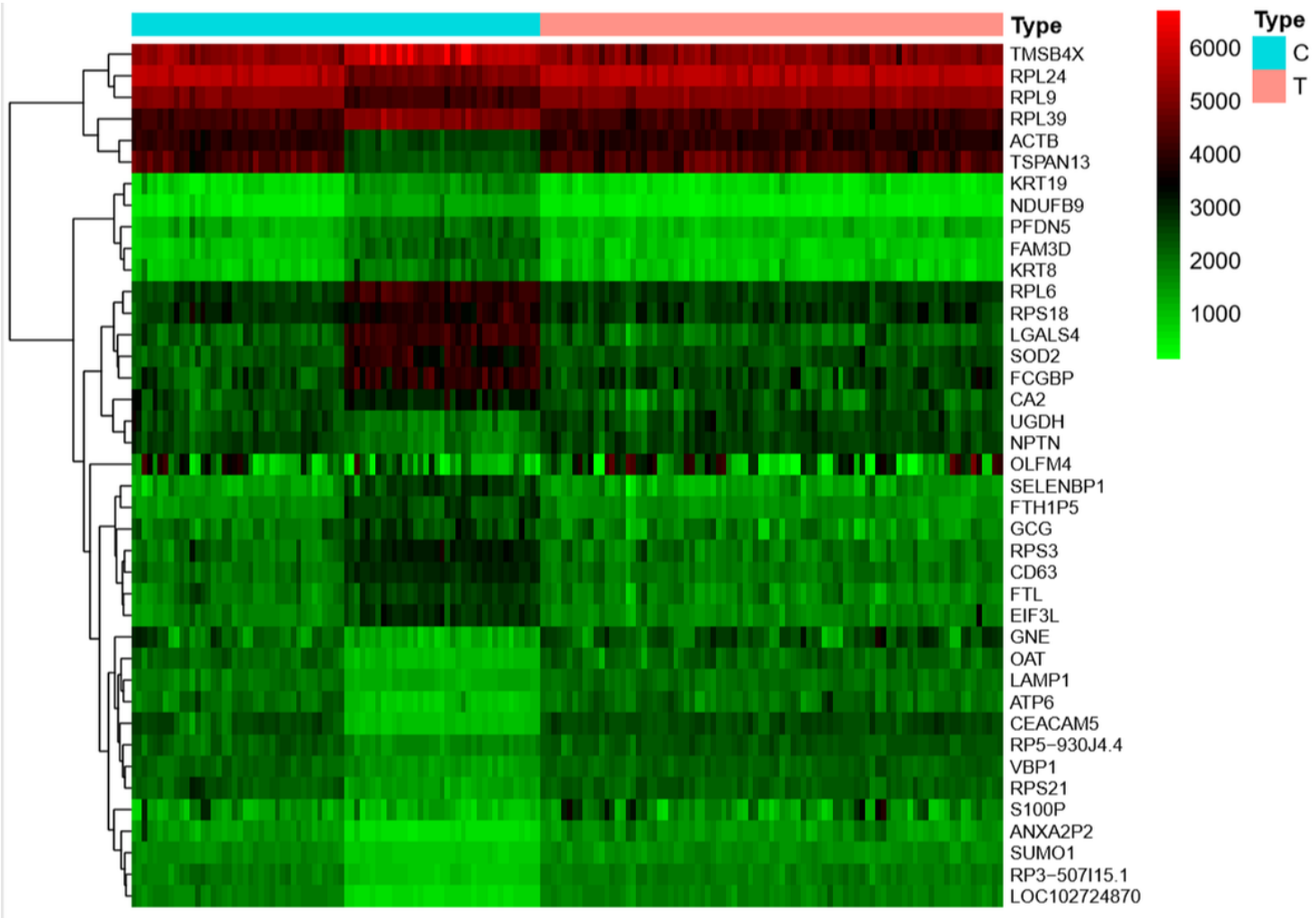

Figure 1

heatmap of difference analysis from GES36701

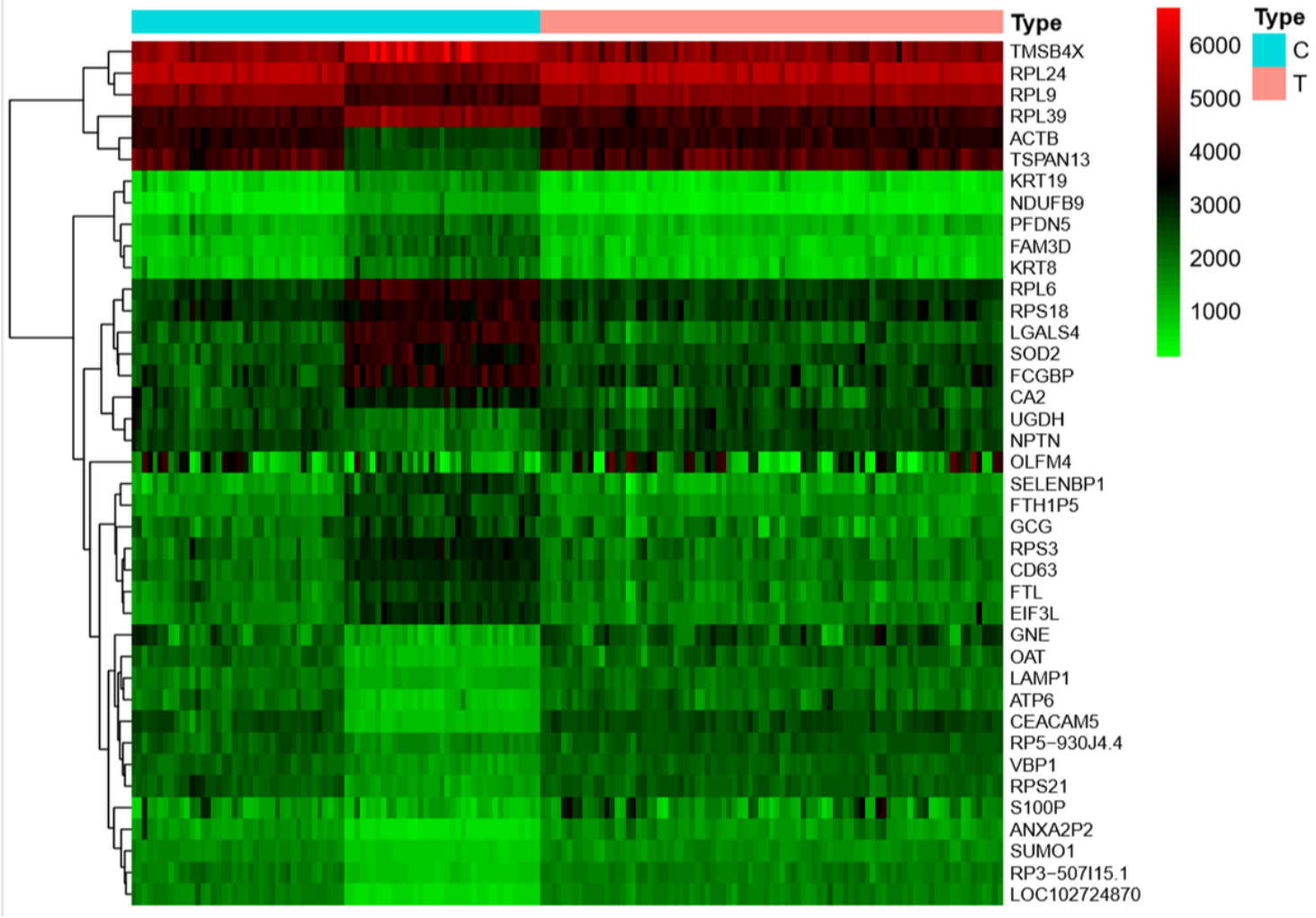

Figure 1

heatmap of difference analysis from GES36701

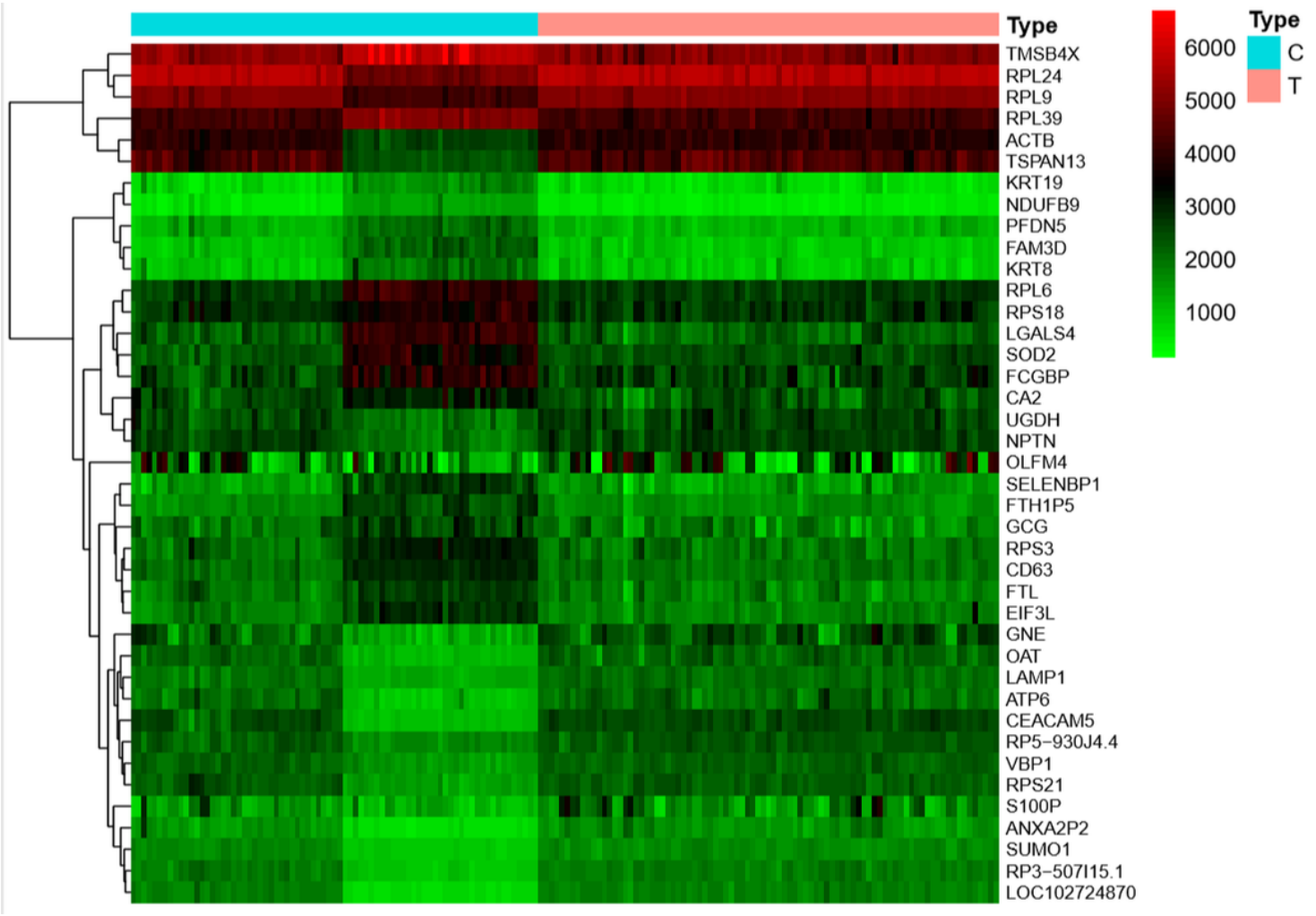

Figure 1

heatmap of difference analysis from GES36701

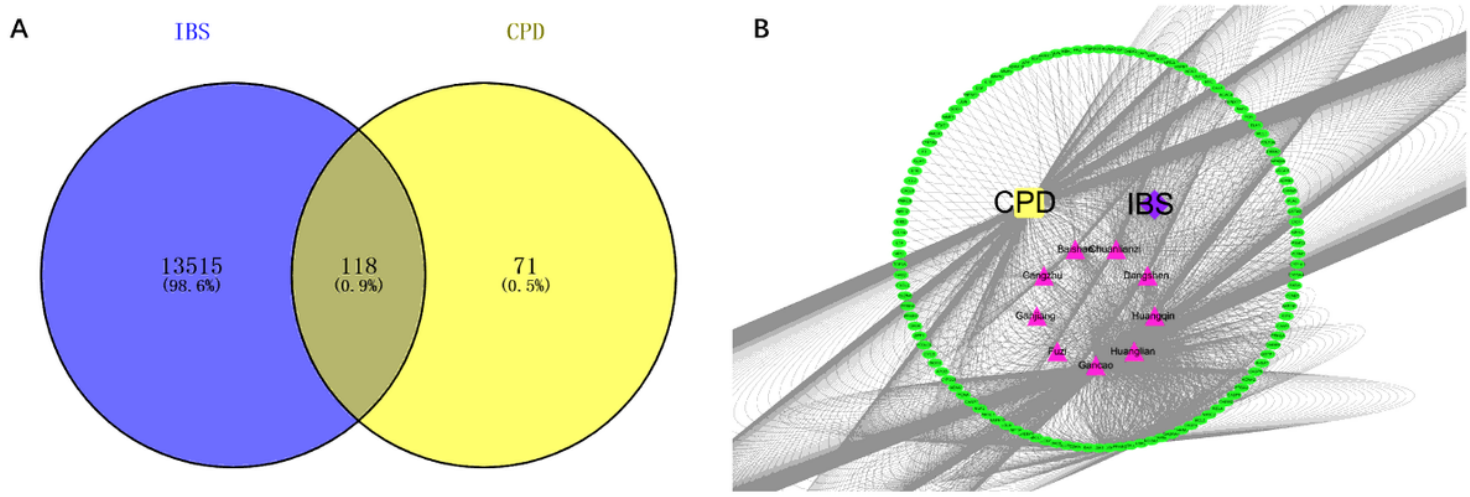

Figure 2

A total of 118 targets were screened at the intersection of CPD and IBS (A). CPD-IBS disease network. Red triangle represent the drug composition of CPD, green circles are potential targets of CPD for the treatment of IBS (B).

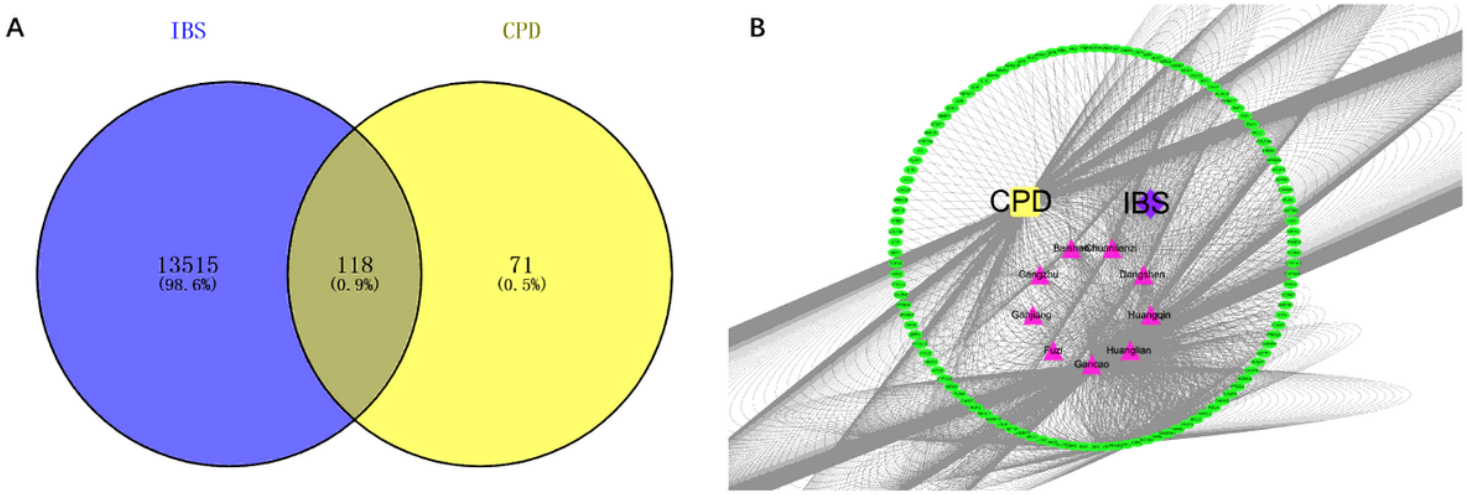

Figure 2

A total of 118 targets were screened at the intersection of CPD and IBS (A). CPD-IBS disease network. Red triangle represent the drug composition of CPD, green circles are potential targets of CPD for the treatment of IBS (B).

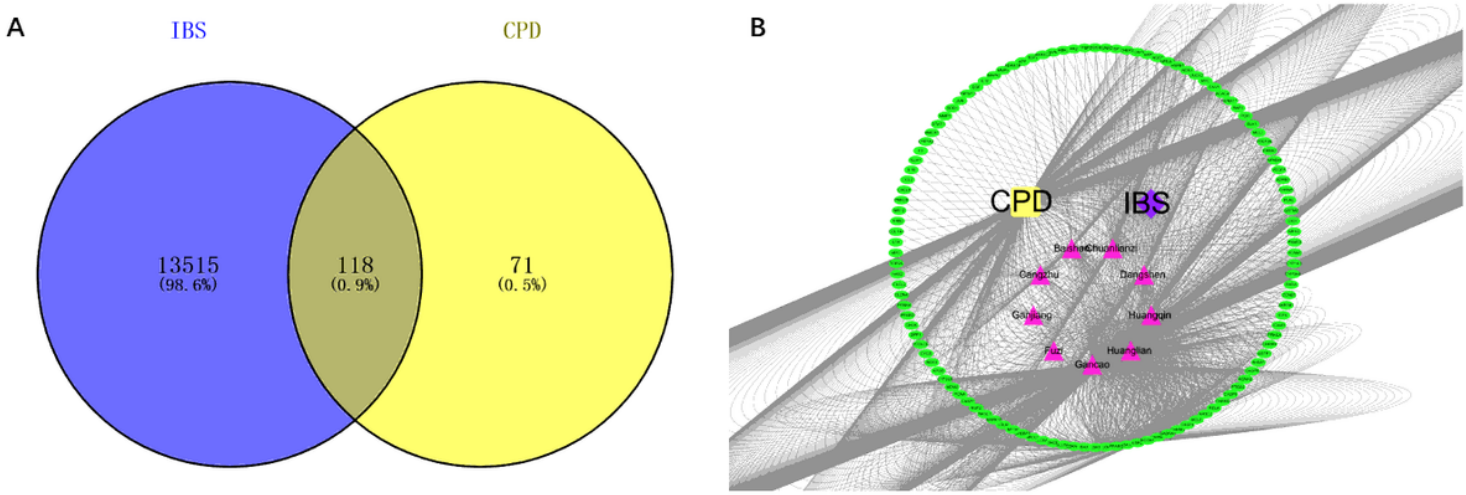

Figure 2

A total of 118 targets were screened at the intersection of CPD and IBS (A). CPD-IBS disease network. Red triangle represent the drug composition of CPD, green circles are potential targets of CPD for the

treatment of IBS (B).

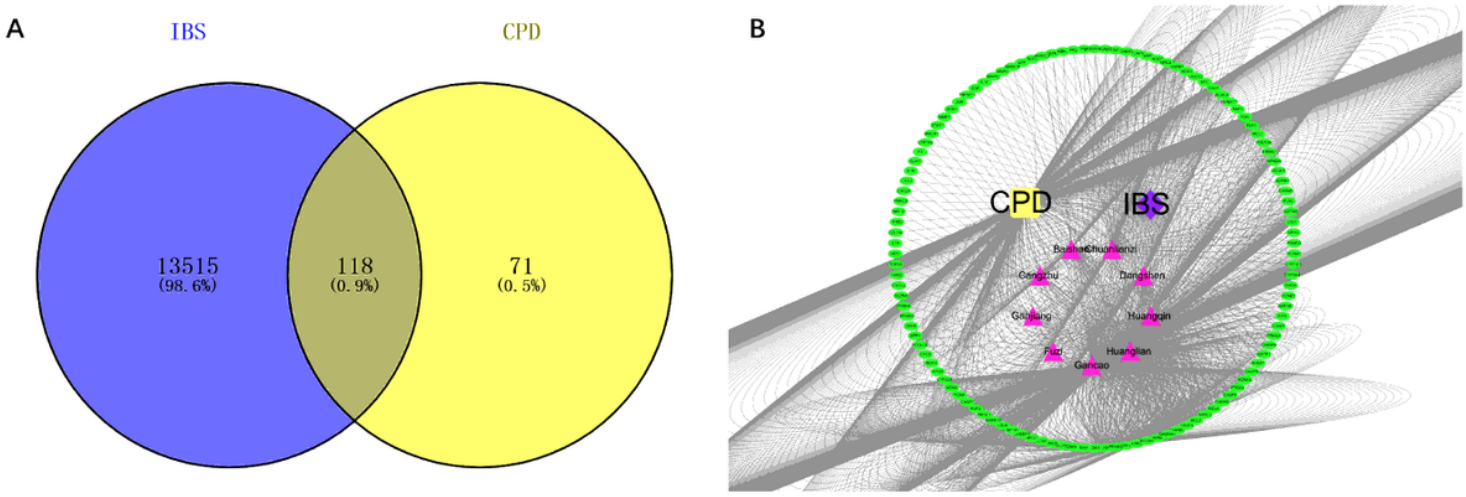

Figure 2

A total of 118 targets were screened at the intersection of CPD and IBS (A). CPD-IBS disease network. Red triangle represent the drug composition of CPD, green circles are potential targets of CPD for the treatment of IBS (B).

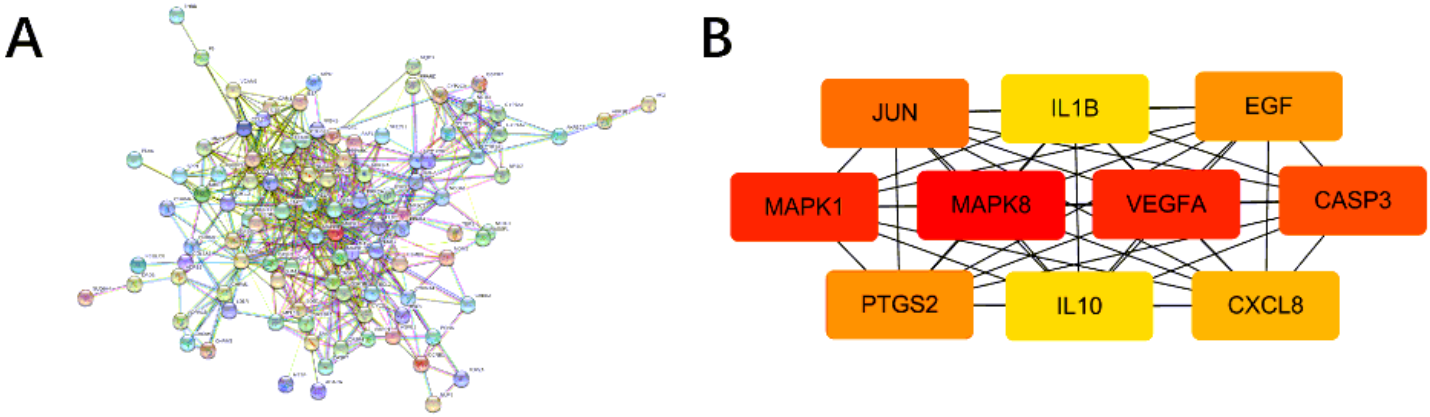

Figure 3

PPI network (A) and core protein of the PPI network (B)

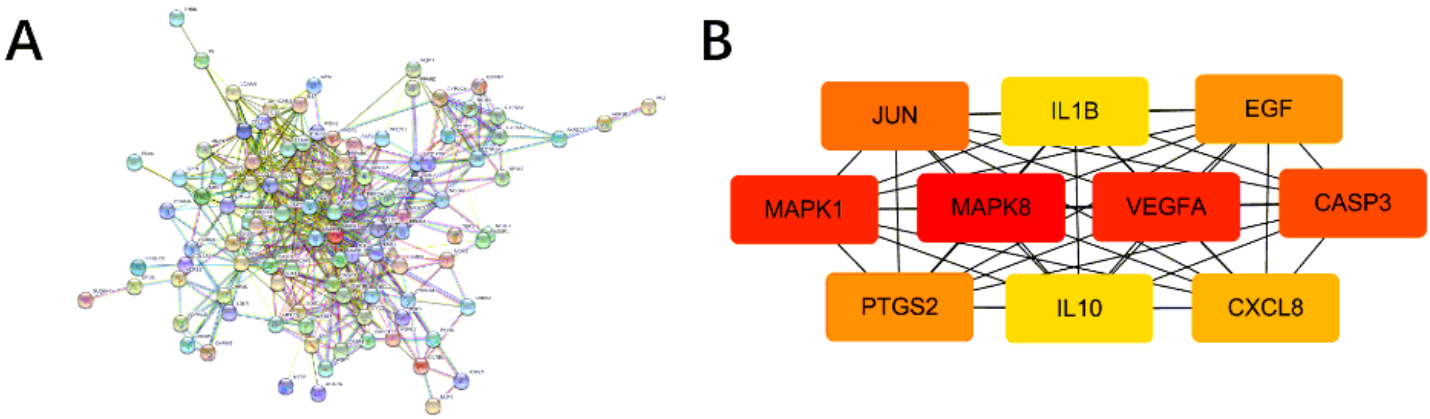

Figure 3

PPI network (A) and core protein of the PPI network (B)

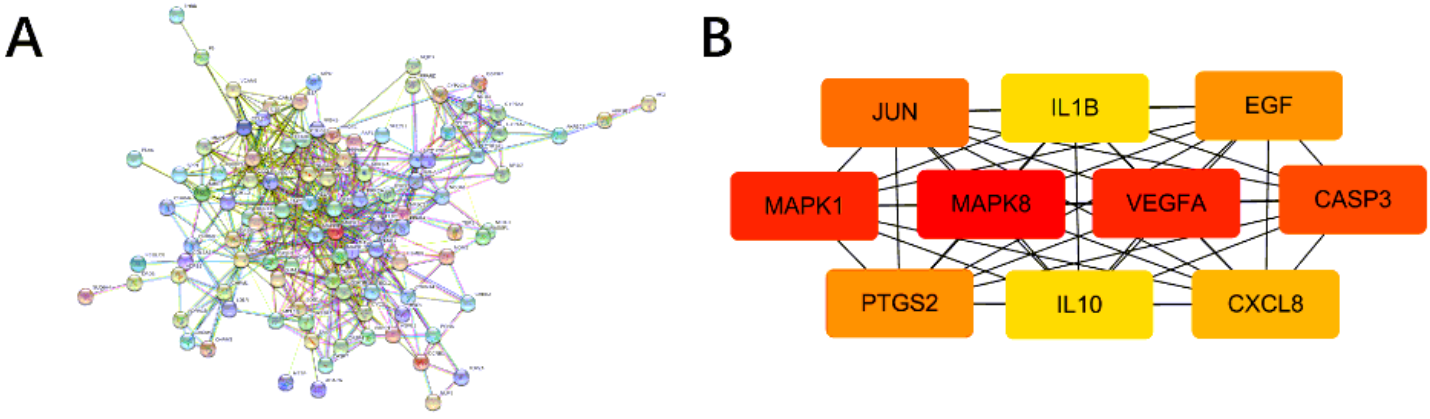

Figure 3

PPI network (A) and core protein of the PPI network (B)

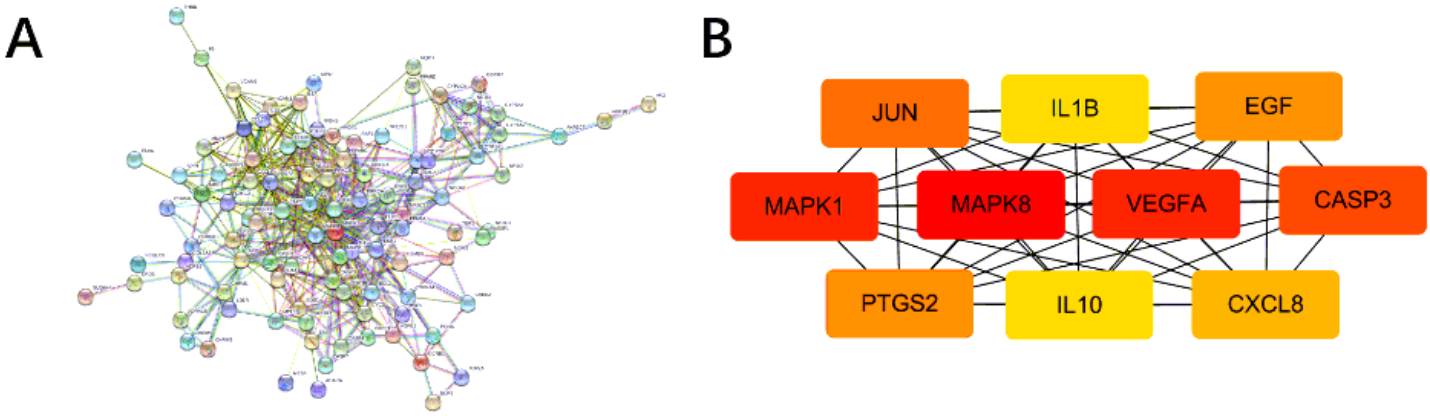

Figure 3

PPI network (A) and core protein of the PPI network (B)

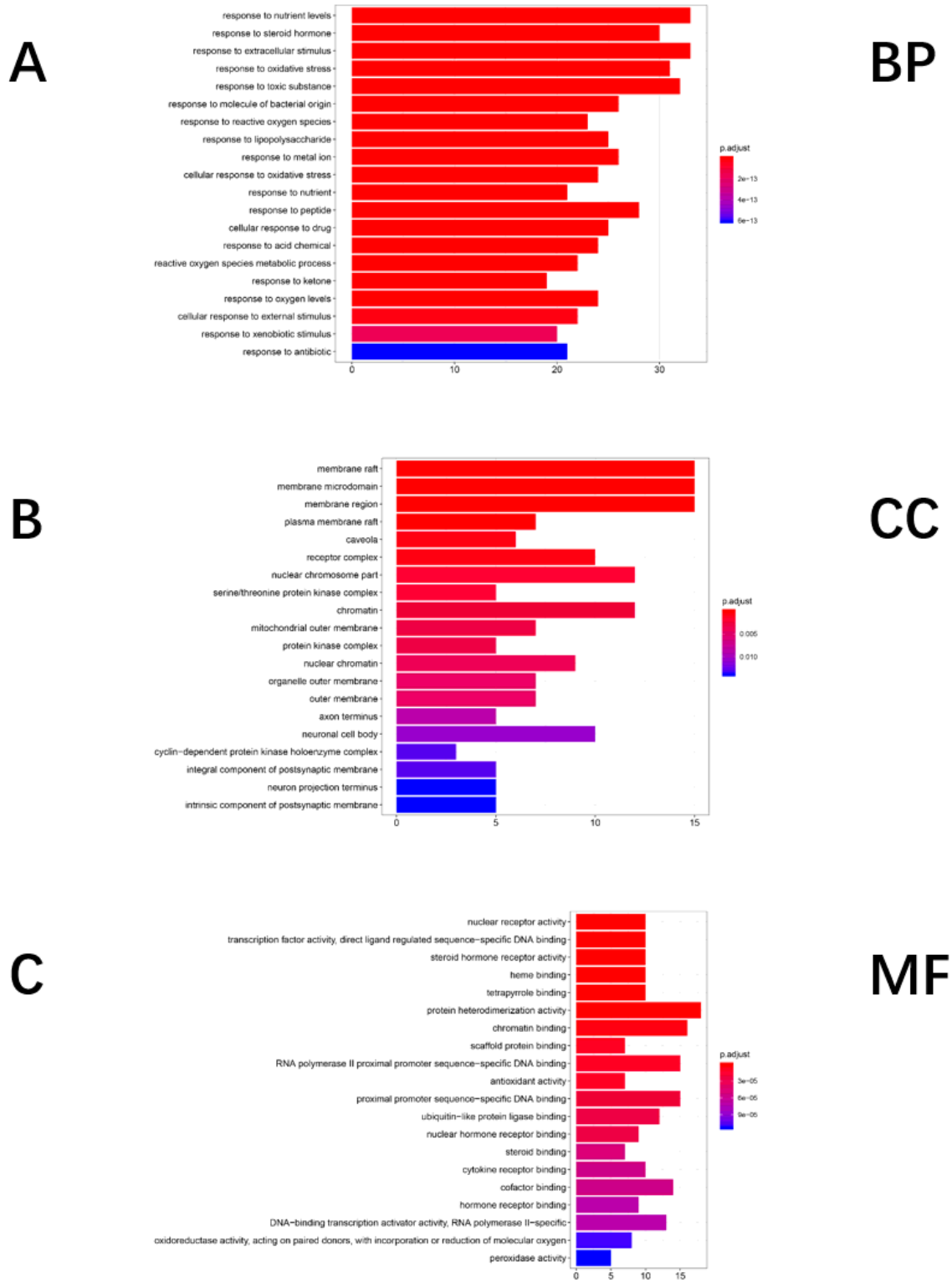

Figure 4

The result of Gene Ontology (GO)enrichment analysis including biological process (A) cellular component (B) molecular function (C)

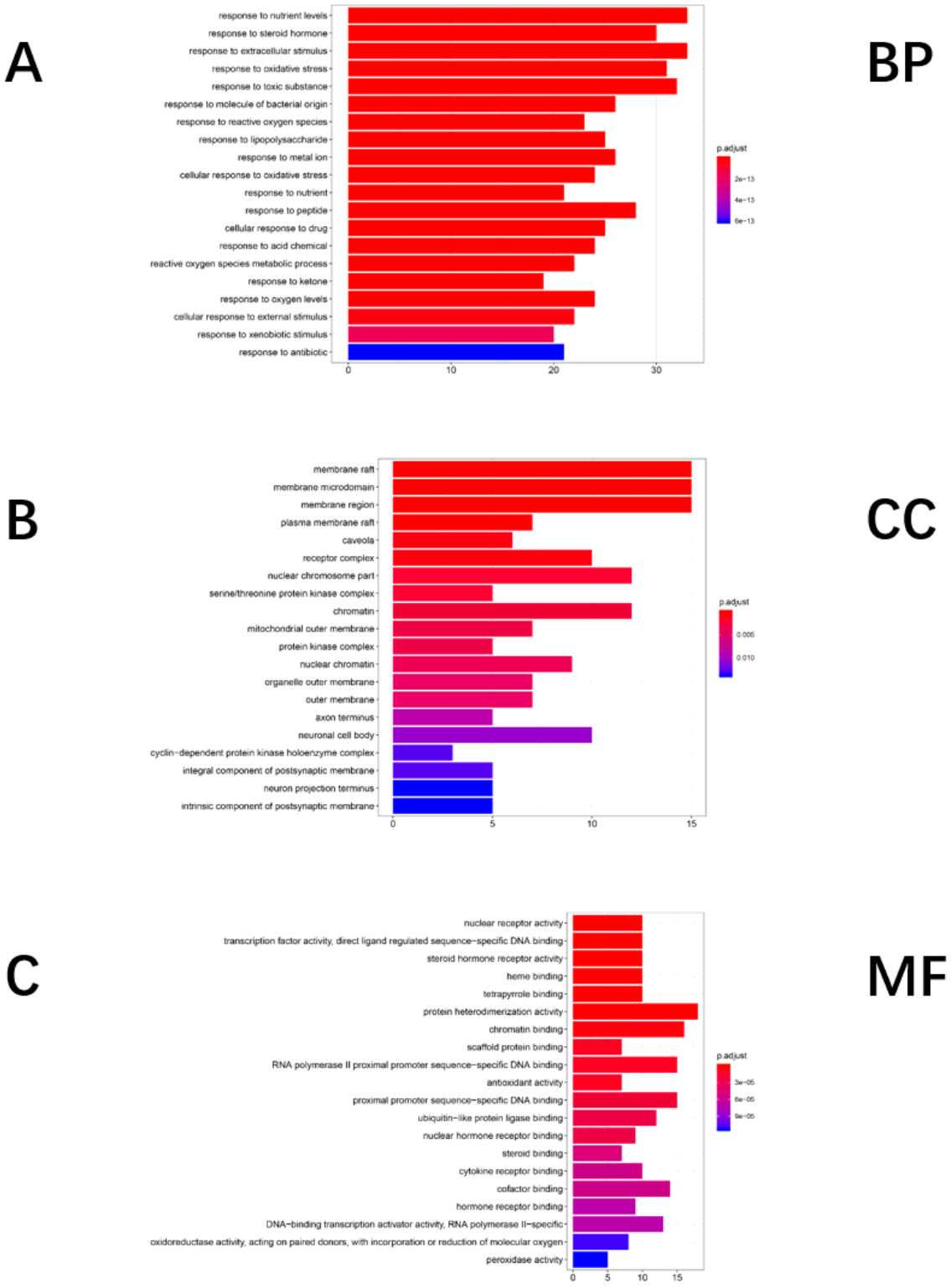

Figure 4

The result of Gene Ontology (GO)enrichment analysis including biological process (A) cellular component (B) molecular function (C)

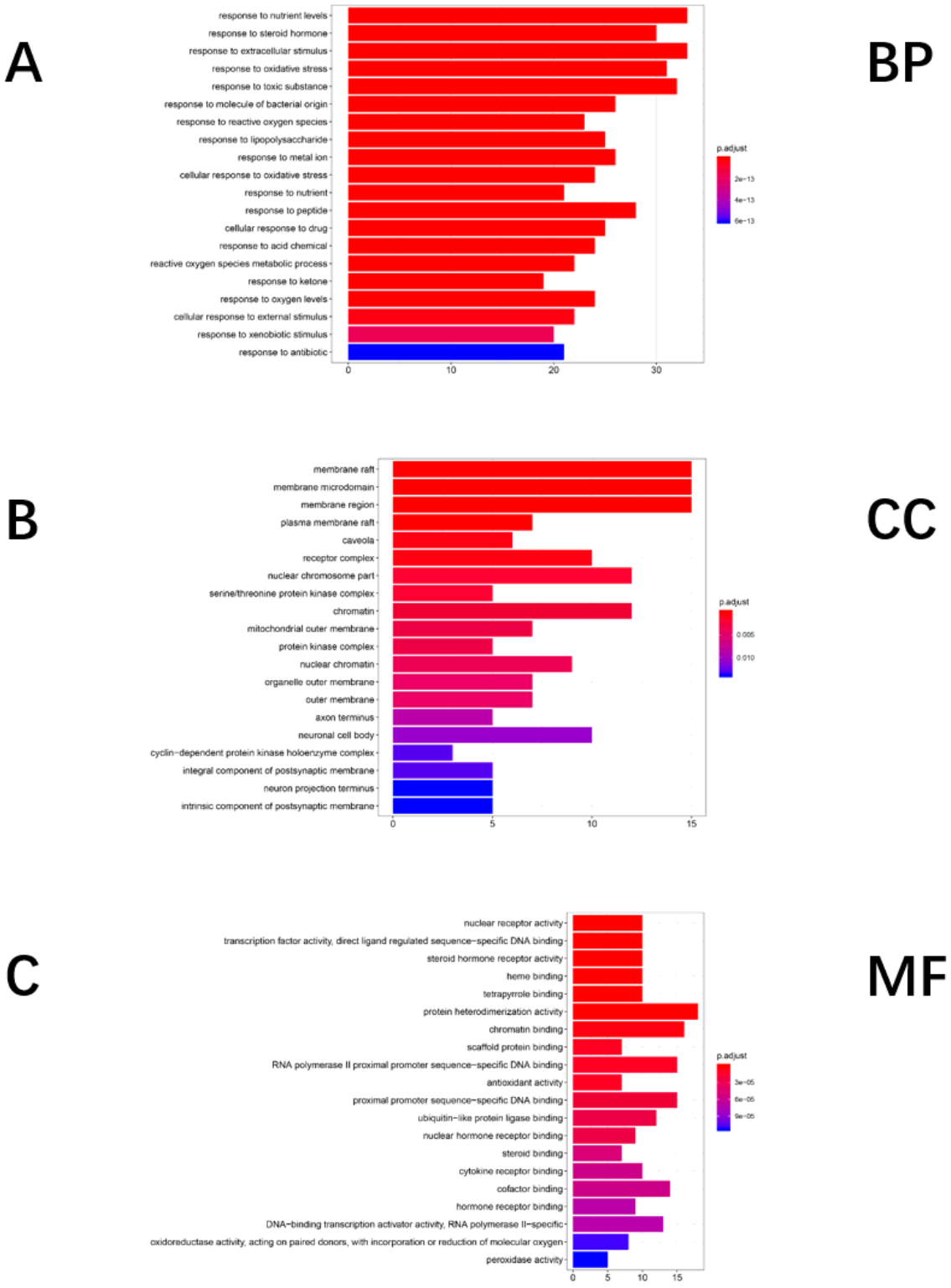

Figure 4

The result of Gene Ontology (GO)enrichment analysis including biological process (A) cellular component (B) molecular function (C)

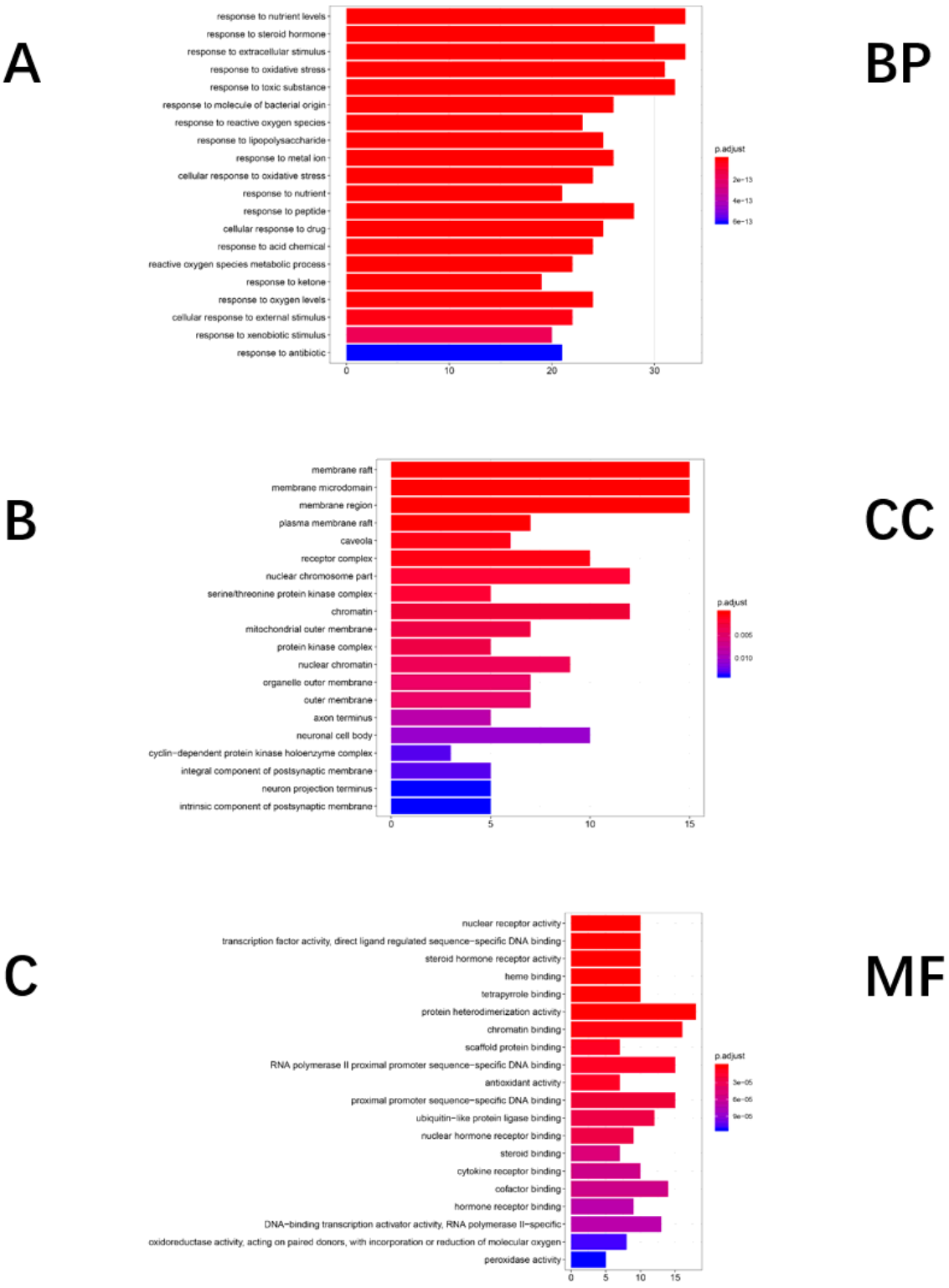

Figure 4

The result of Gene Ontology (GO)enrichment analysis including biological process (A) cellular component (B) molecular function (C)

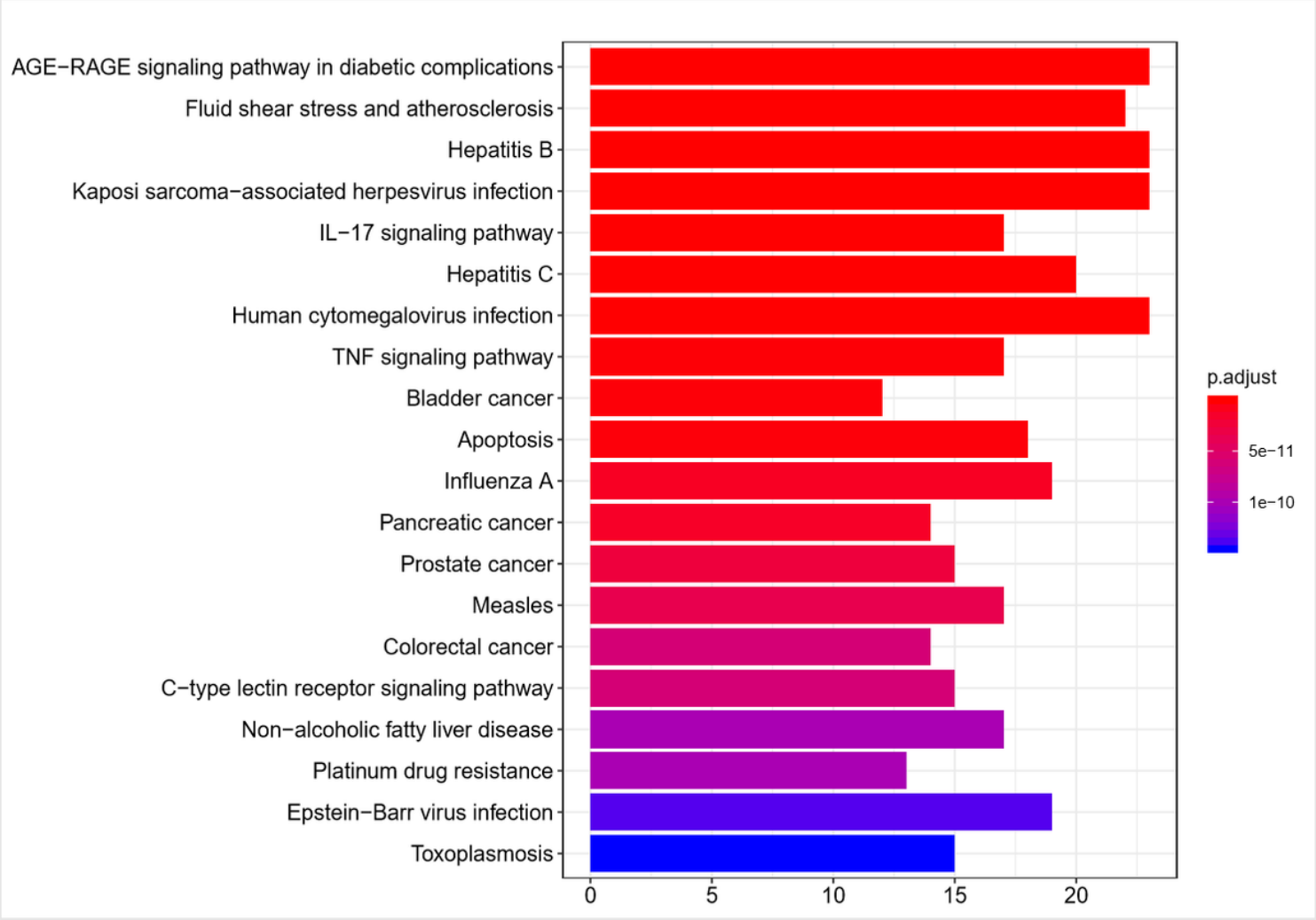

Figure 5

the result of KEGG pathway enrichment analysis

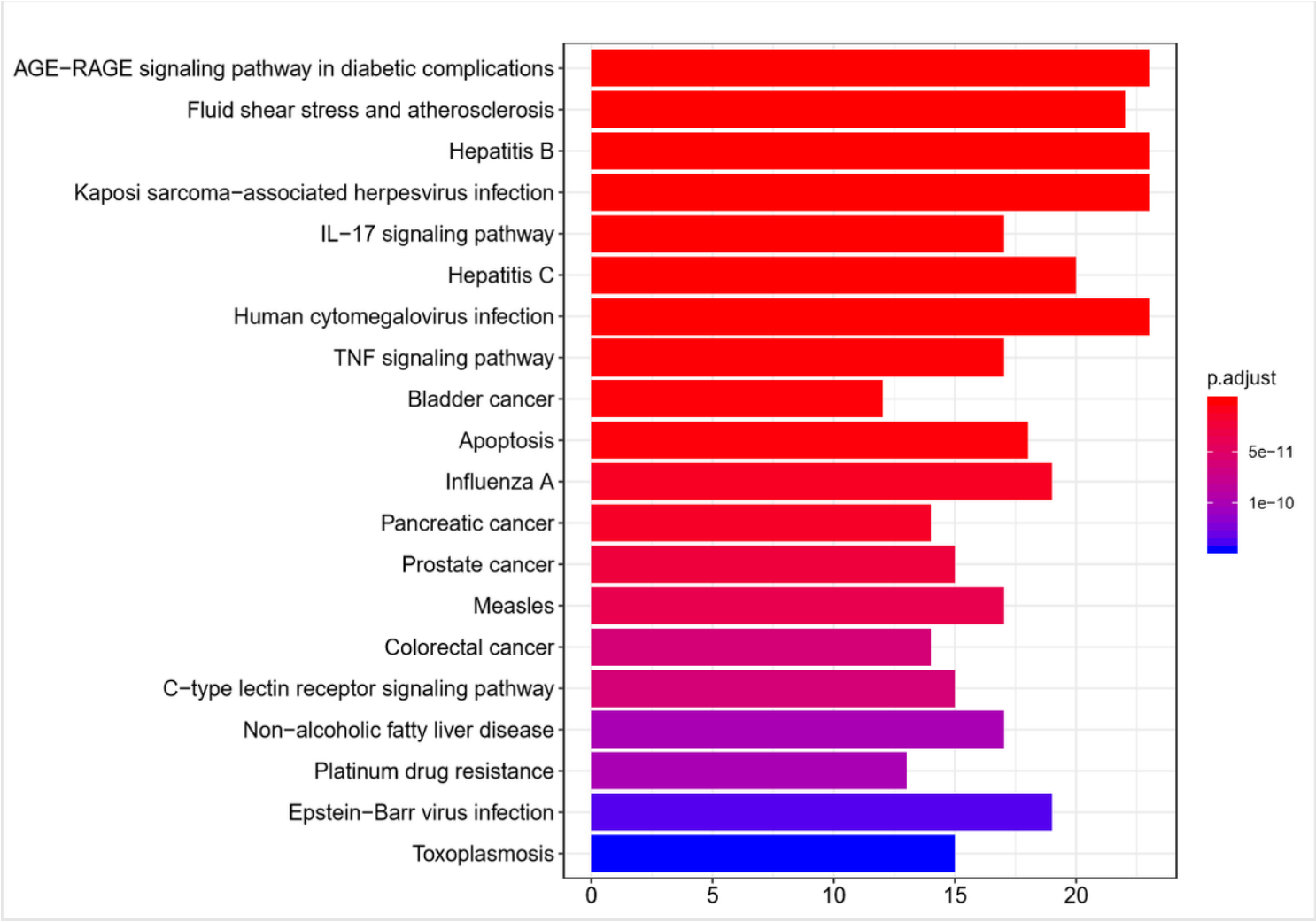

Figure 5

the result of KEGG pathway enrichment analysis

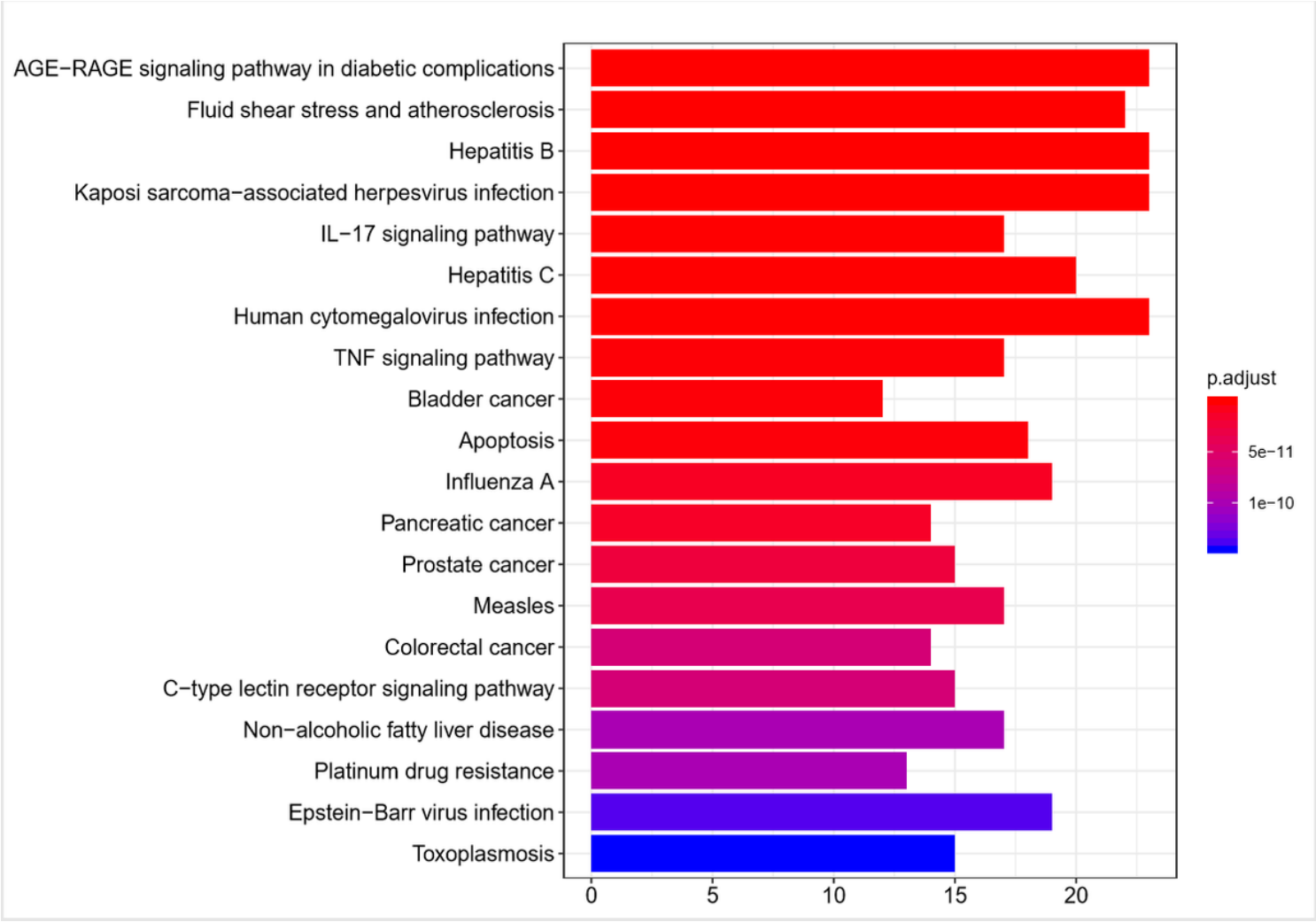

Figure 5

the result of KEGG pathway enrichment analysis

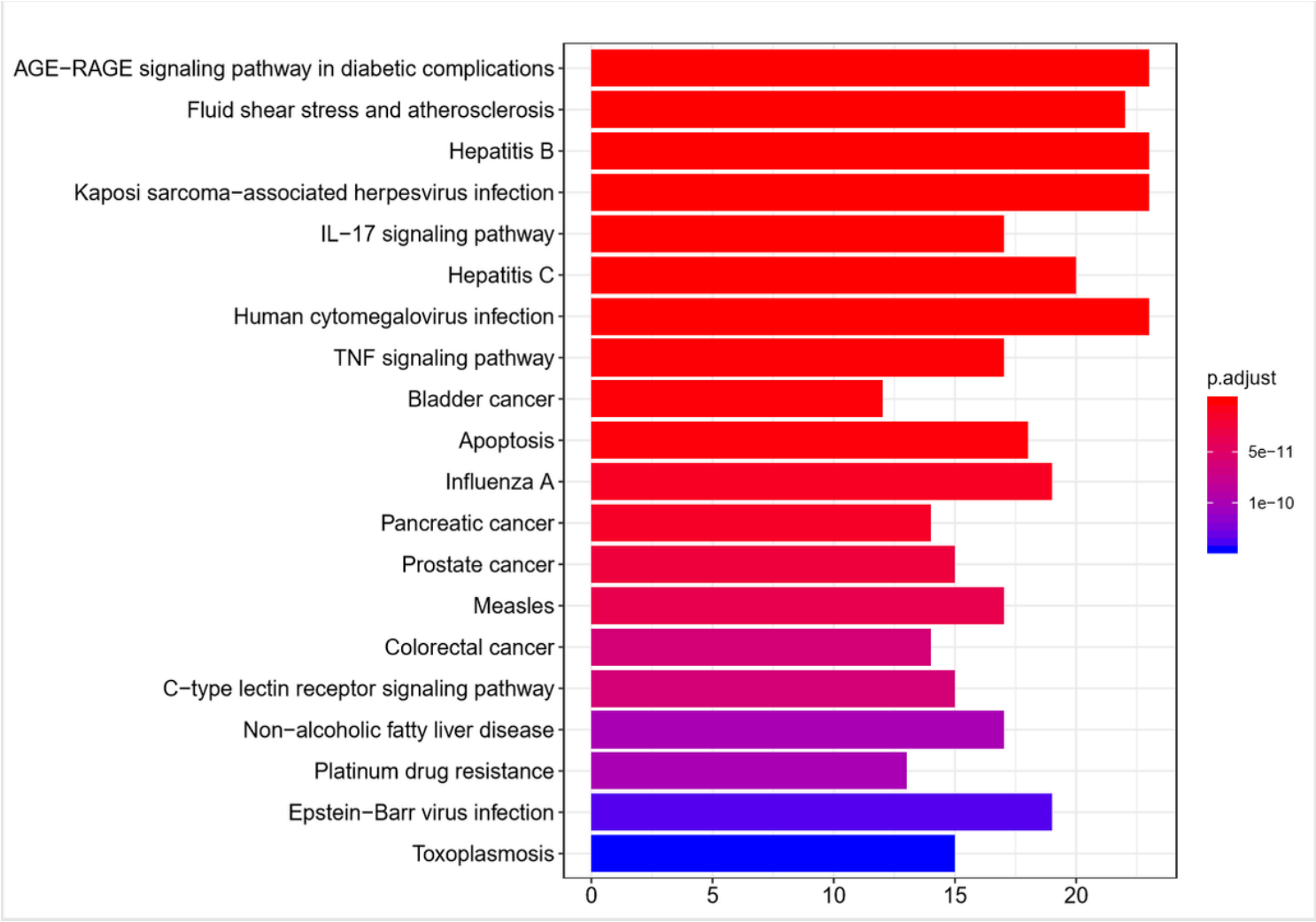

Figure 5

the result of KEGG pathway enrichment analysis

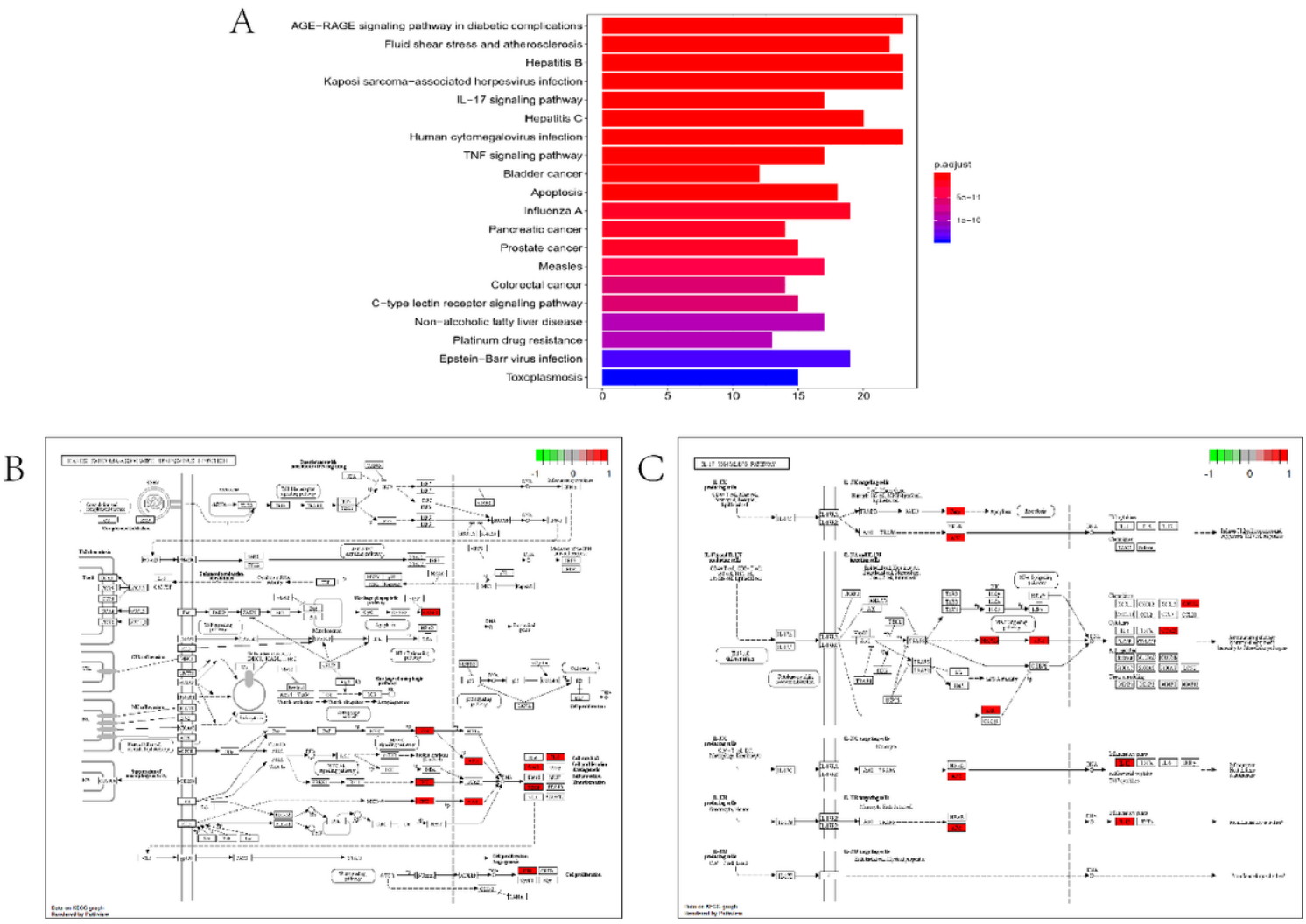

Figure 6

the result of enrichment analysis of the core 10 proteins (A). The signaling pathway picture of Kaposi sarcoma-associated herpesvirus infection (B) and IL-17 signaling pathway (C).

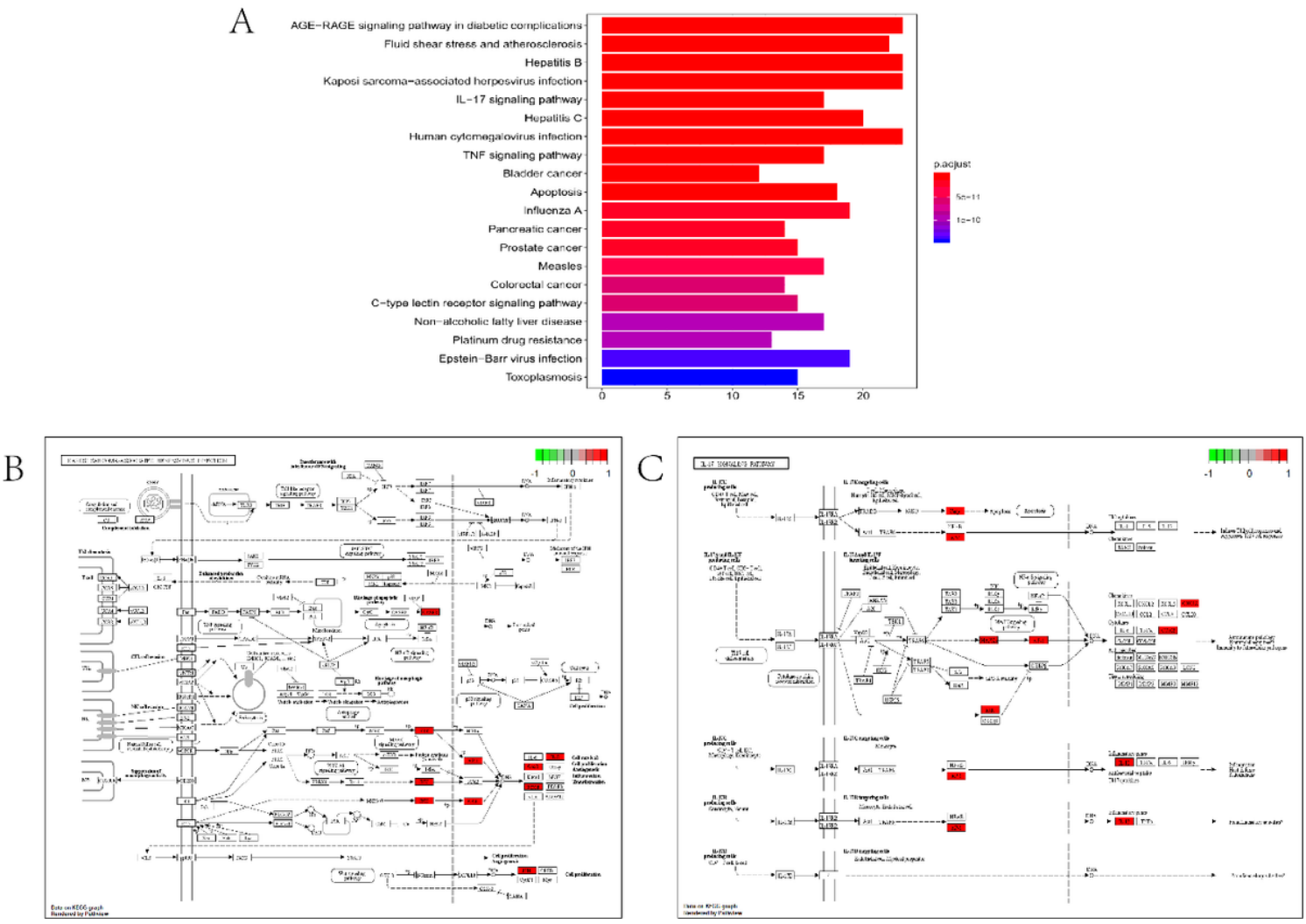

Figure 6

the result of enrichment analysis of the core 10 proteins (A). The signaling pathway picture of Kaposi sarcoma-associated herpesvirus infection (B) and IL-17 signaling pathway (C).

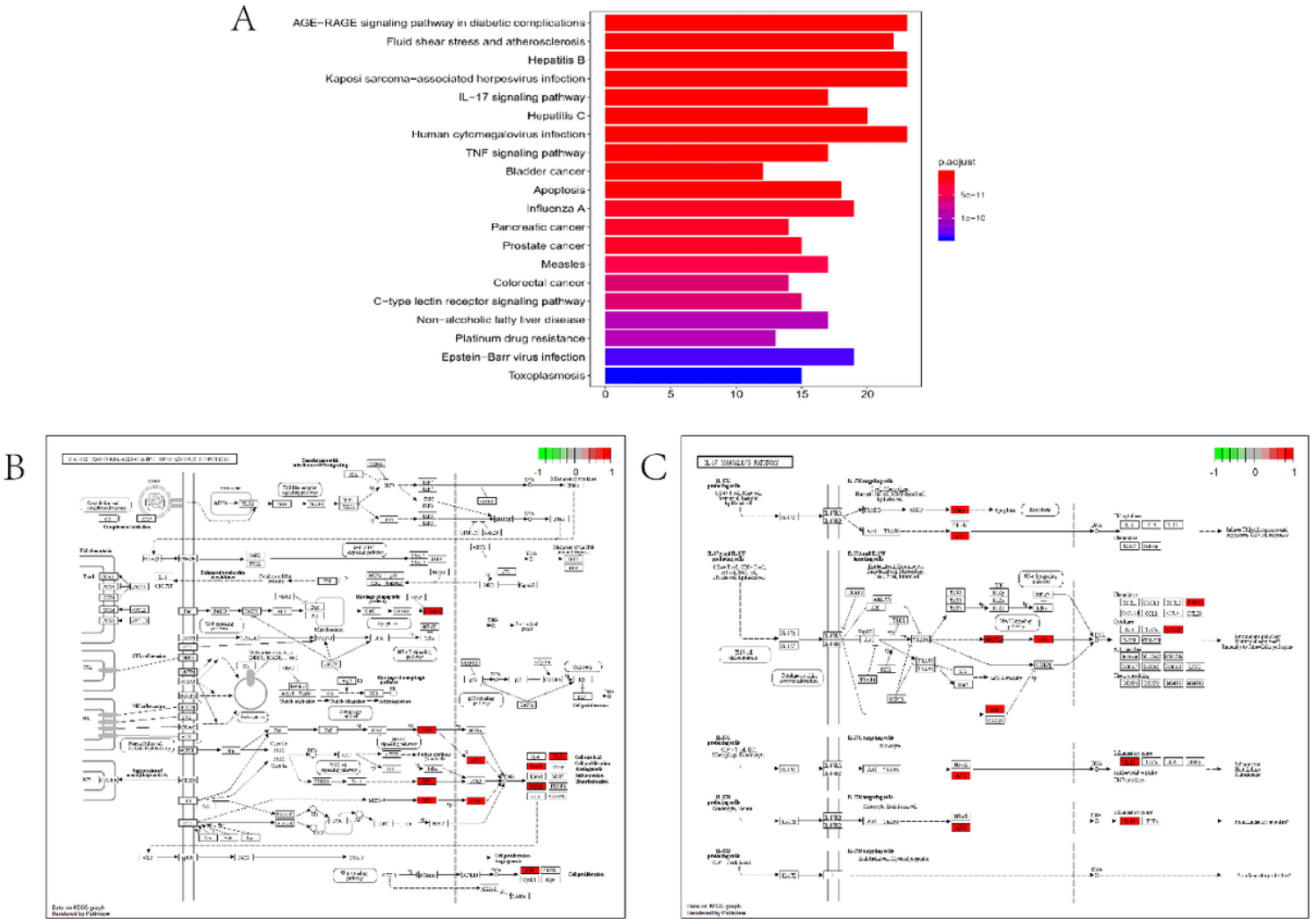

Figure 6

the result of enrichment analysis of the core 10 proteins (A). The signaling pathway picture of Kaposi sarcoma-associated herpesvirus infection (B) and IL-17 signaling pathway (C).

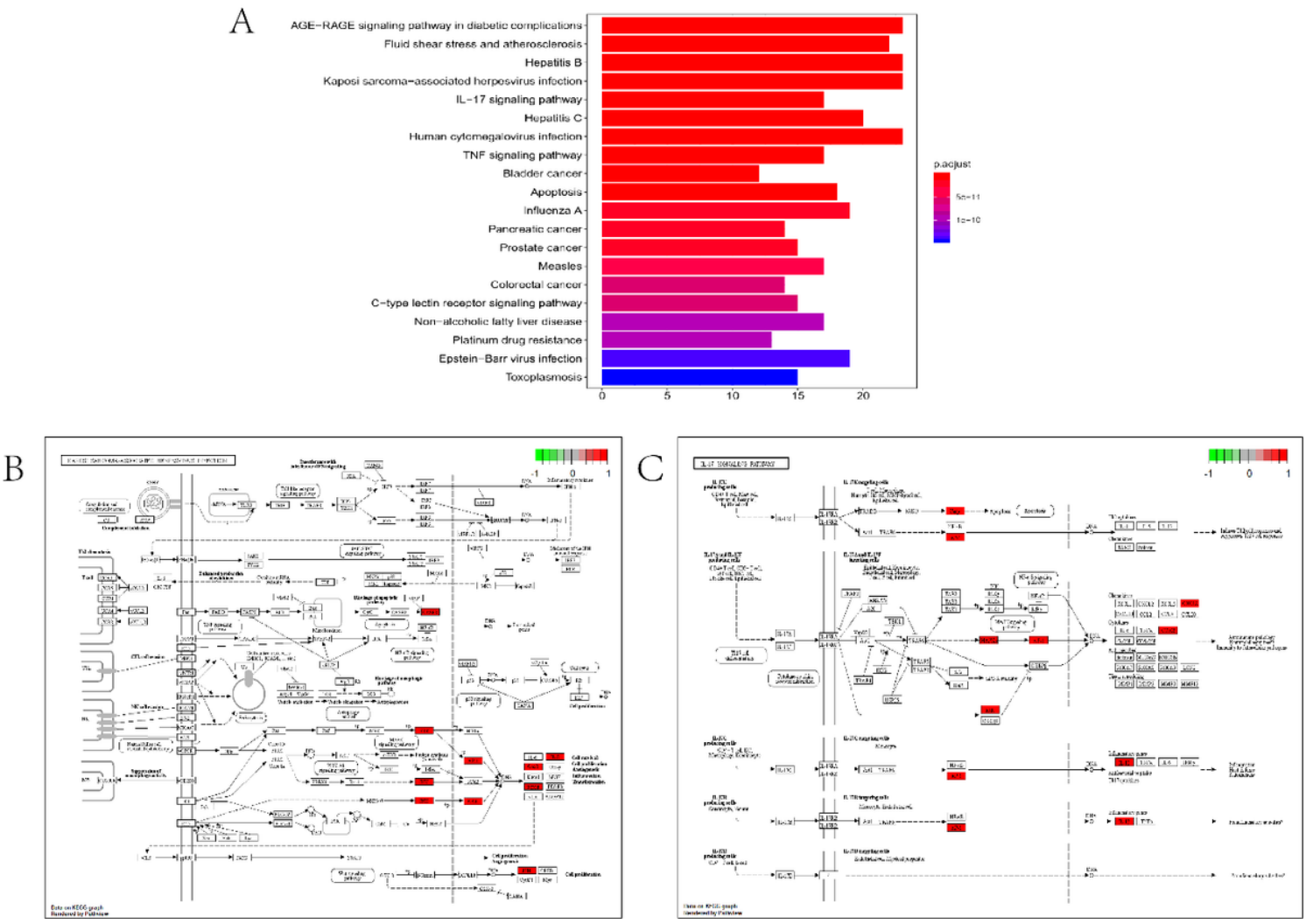

Figure 6

the result of enrichment analysis of the core 10 proteins (A). The signaling pathway picture of Kaposi sarcoma-associated herpesvirus infection (B) and IL-17 signaling pathway (C).

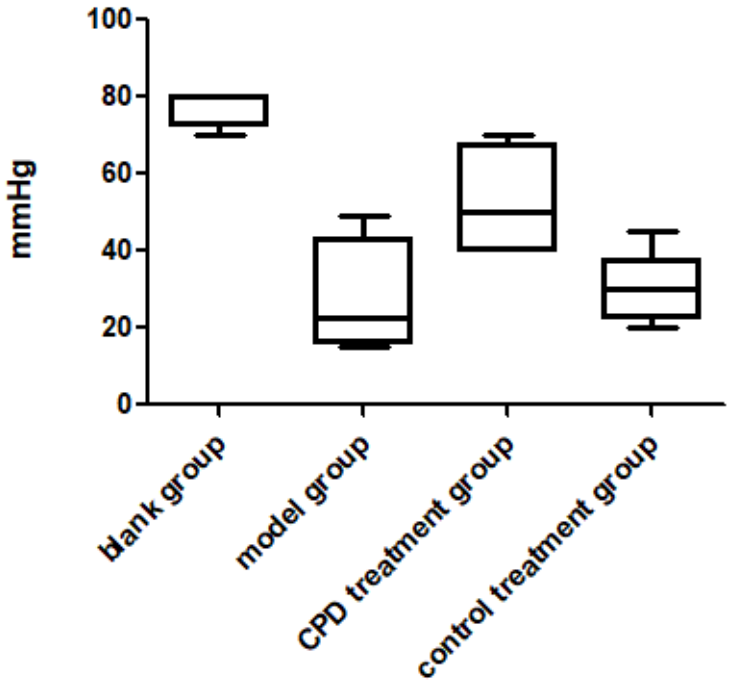

Figure 7

The rats in the model group and the control treatment group have obvious visceral pain threshold at 20-40mmHG. The CPD treatment group will have a visceral pain threshold at 40-70mmHg. Visceral pain threshold occurred in the blank group at 80mmHg or greater. $P < 0.0001$.

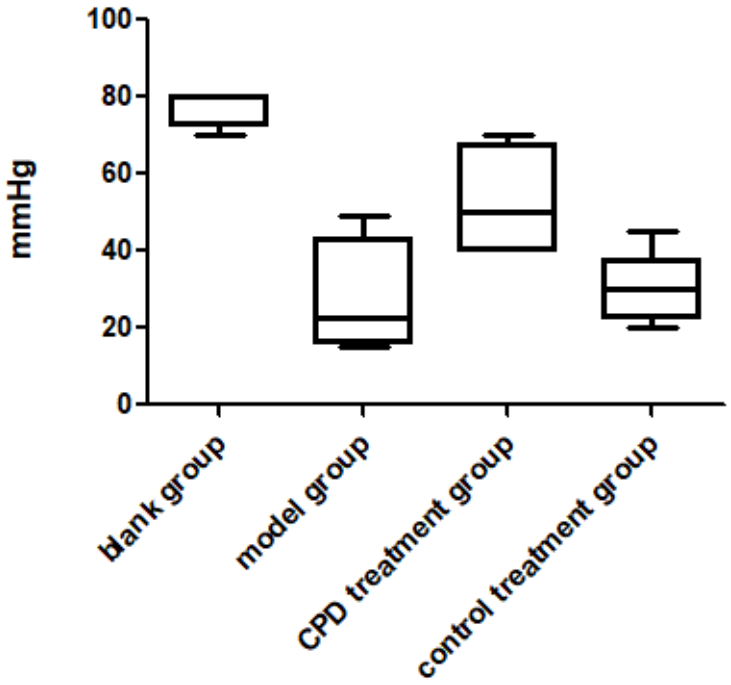

Figure 7

The rats in the model group and the control treatment group have obvious visceral pain threshold at 20-40mmHG. The CPD treatment group will have a visceral pain threshold at 40-70mmHg. Visceral pain threshold occurred in the blank group at 80mmHg or greater. $P < 0.0001$.

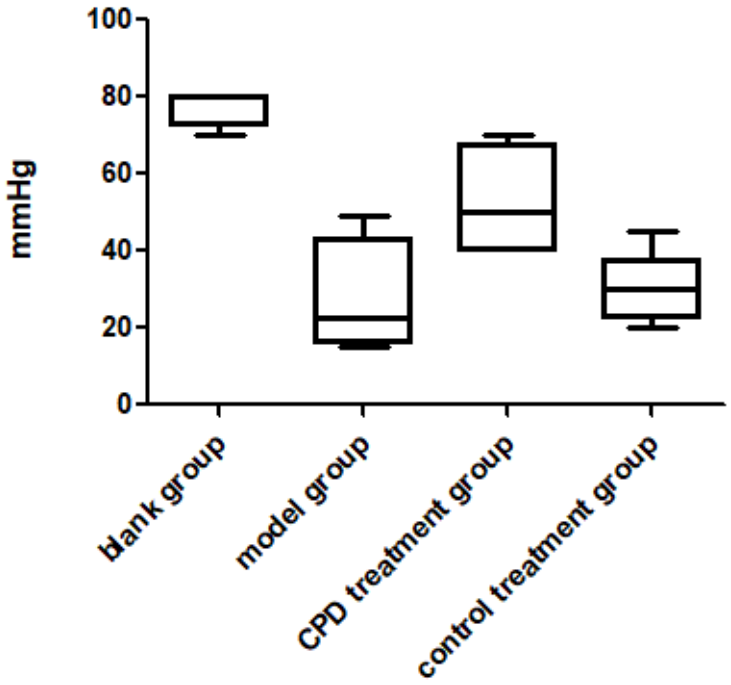

Figure 7

The rats in the model group and the control treatment group have obvious visceral pain threshold at 20-40mmHG. The CPD treatment group will have a visceral pain threshold at 40-70mmHg. Visceral pain threshold occurred in the blank group at 80mmHg or greater. $P < 0.0001$.

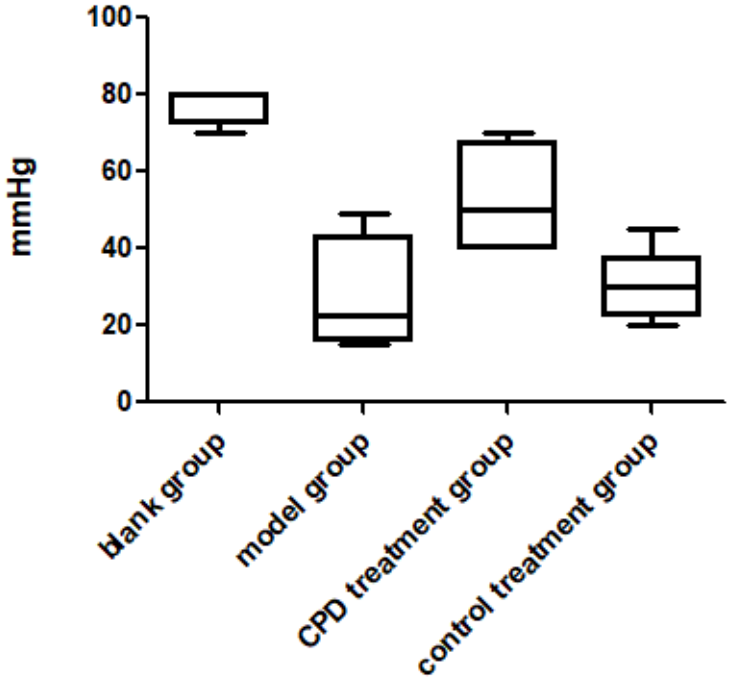

Figure 7

The rats in the model group and the control treatment group have obvious visceral pain threshold at 20-40mmHG. The CPD treatment group will have a visceral pain threshold at 40-70mmHg. Visceral pain threshold occurred in the blank group at 80mmHg or greater. $P < 0.0001$.

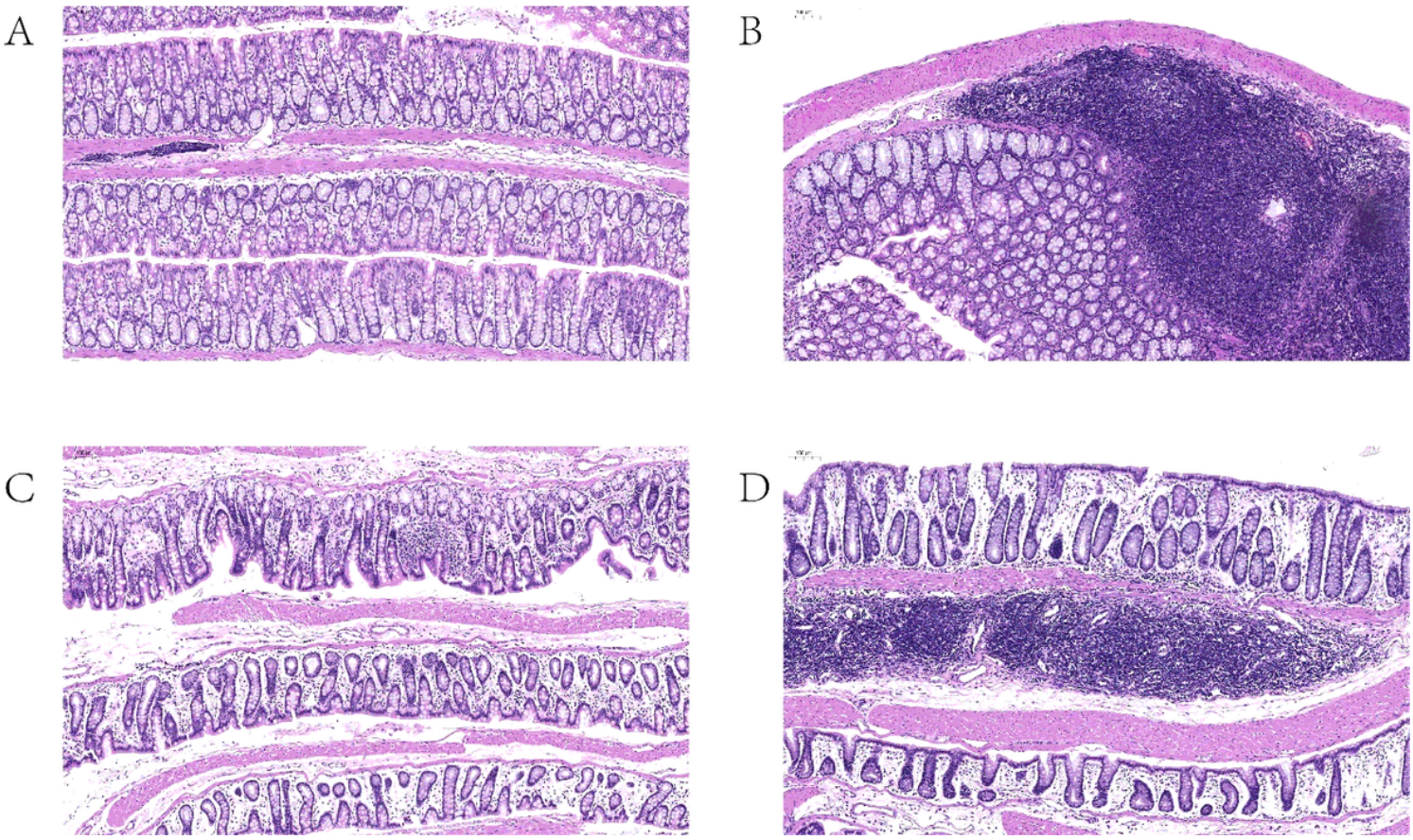

Figure 8

Compare with blank group (A) and CPD treatment group (D), the model group (B) and control treatment group (C) apparent exhibit lymphocyte proliferation.Slides shown (×400 magnification) are representative of common findings.

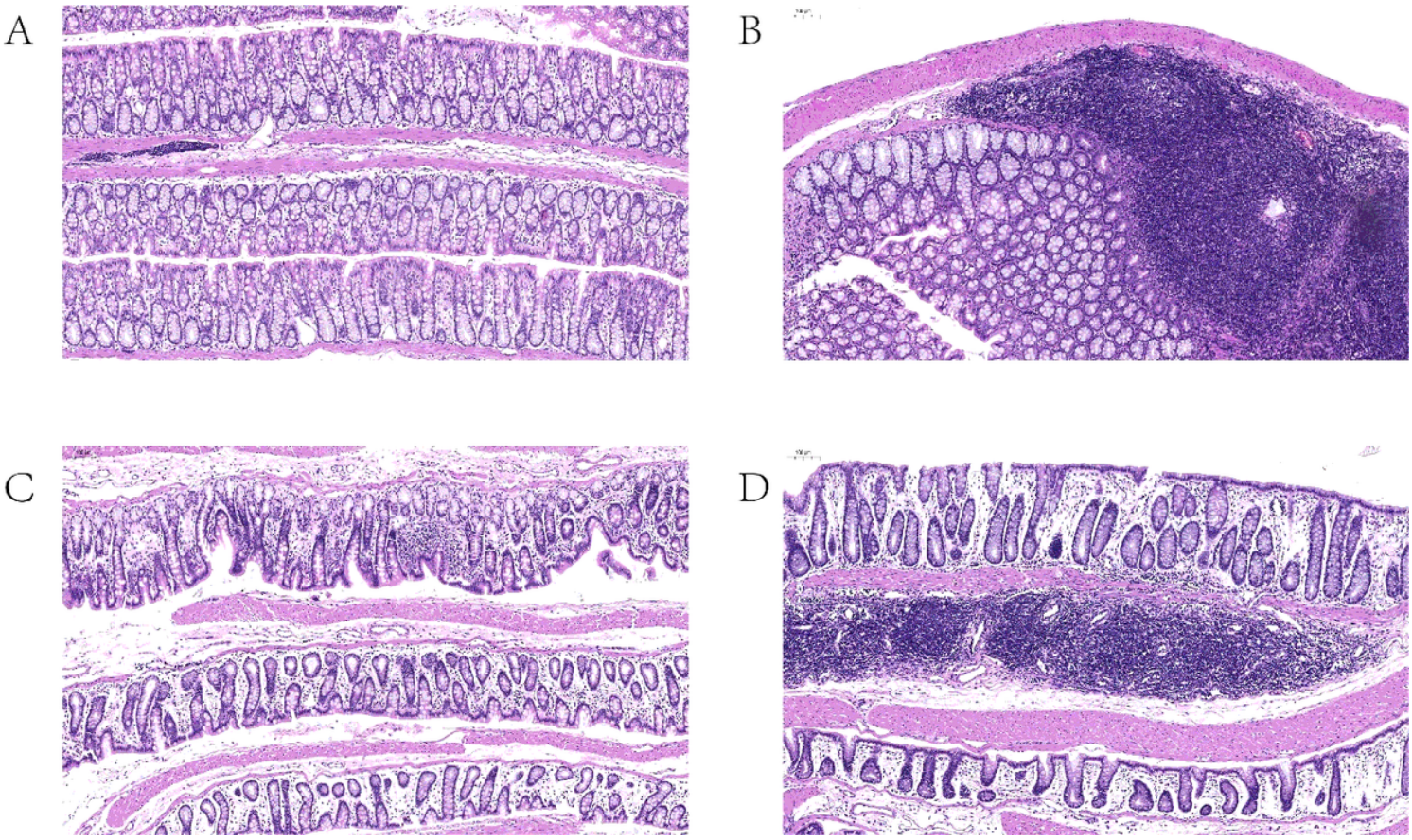

Figure 8

Compare with blank group (A) and CPD treatment group (D), the model group (B) and control treatment group (C) apparent exhibit lymphocyte proliferation.Slides shown (×400 magnification) are representative of common findings.

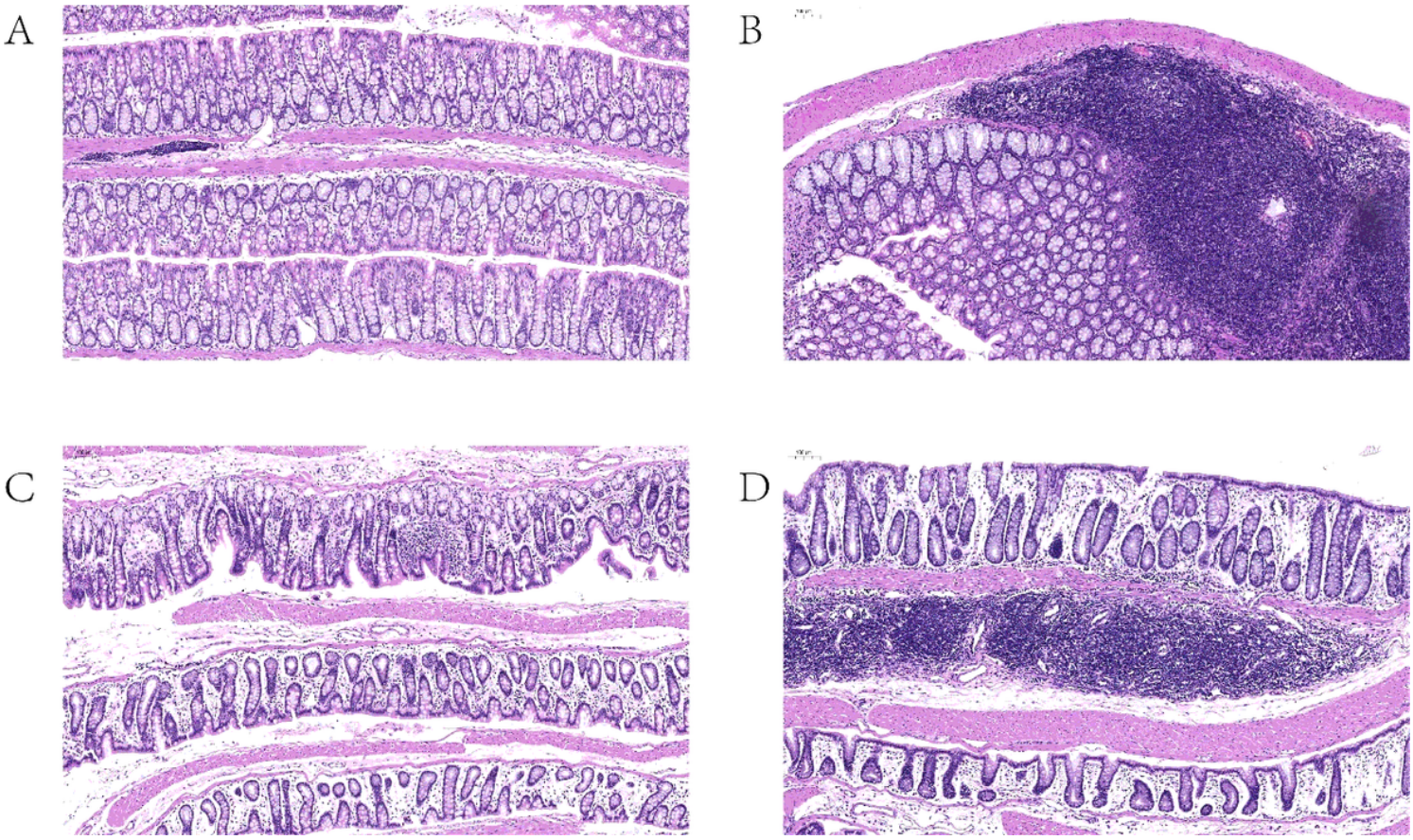

Figure 8

Compare with blank group (A) and CPD treatment group (D), the model group (B) and control treatment group (C) apparent exhibit lymphocyte proliferation.Slides shown (×400 magnification) are representative of common findings.

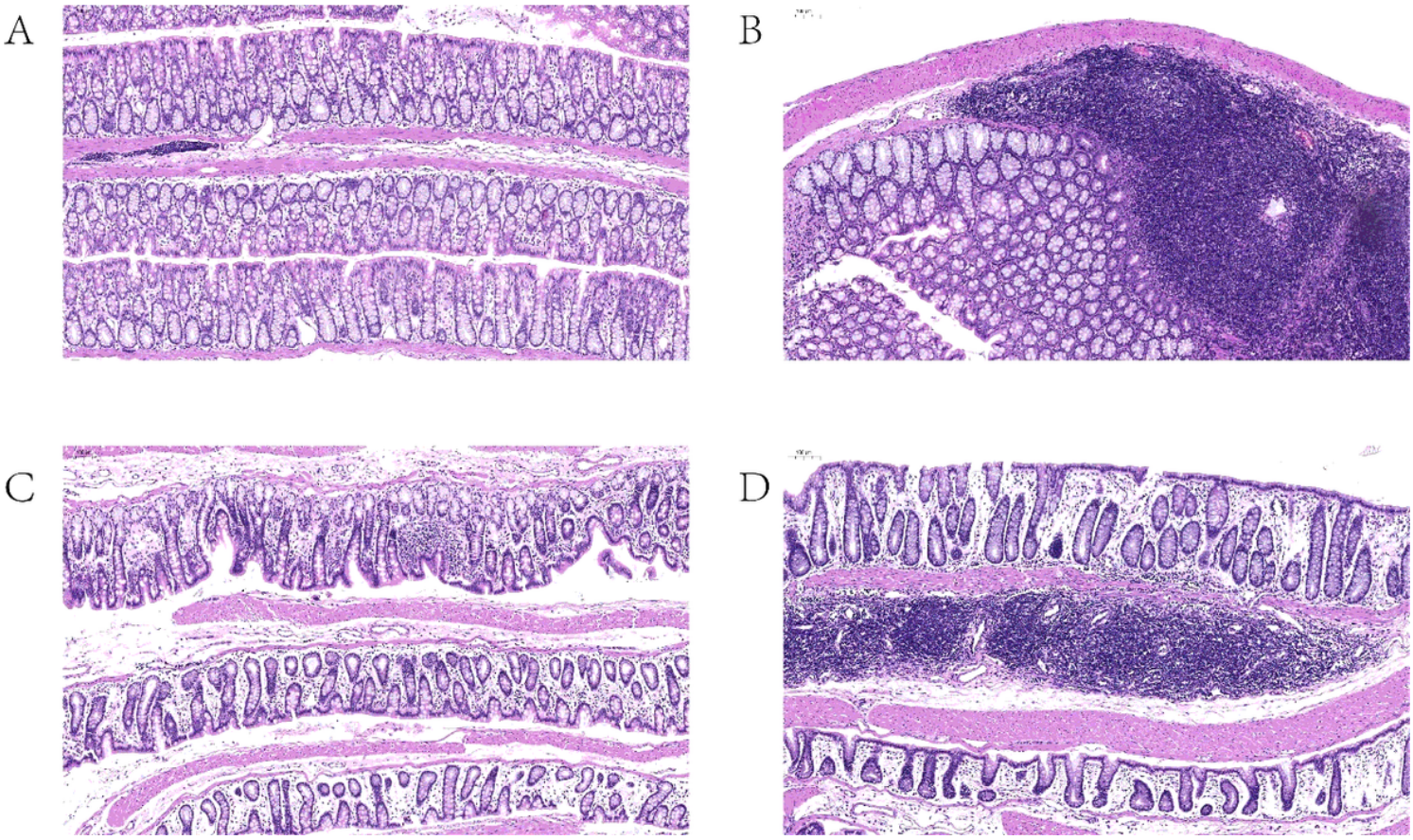

Figure 8

Compare with blank group (A) and CPD treatment group (D), the model group (B) and control treatment group (C) apparent exhibit lymphocyte proliferation.Slides shown (×400 magnification) are representative of common findings.

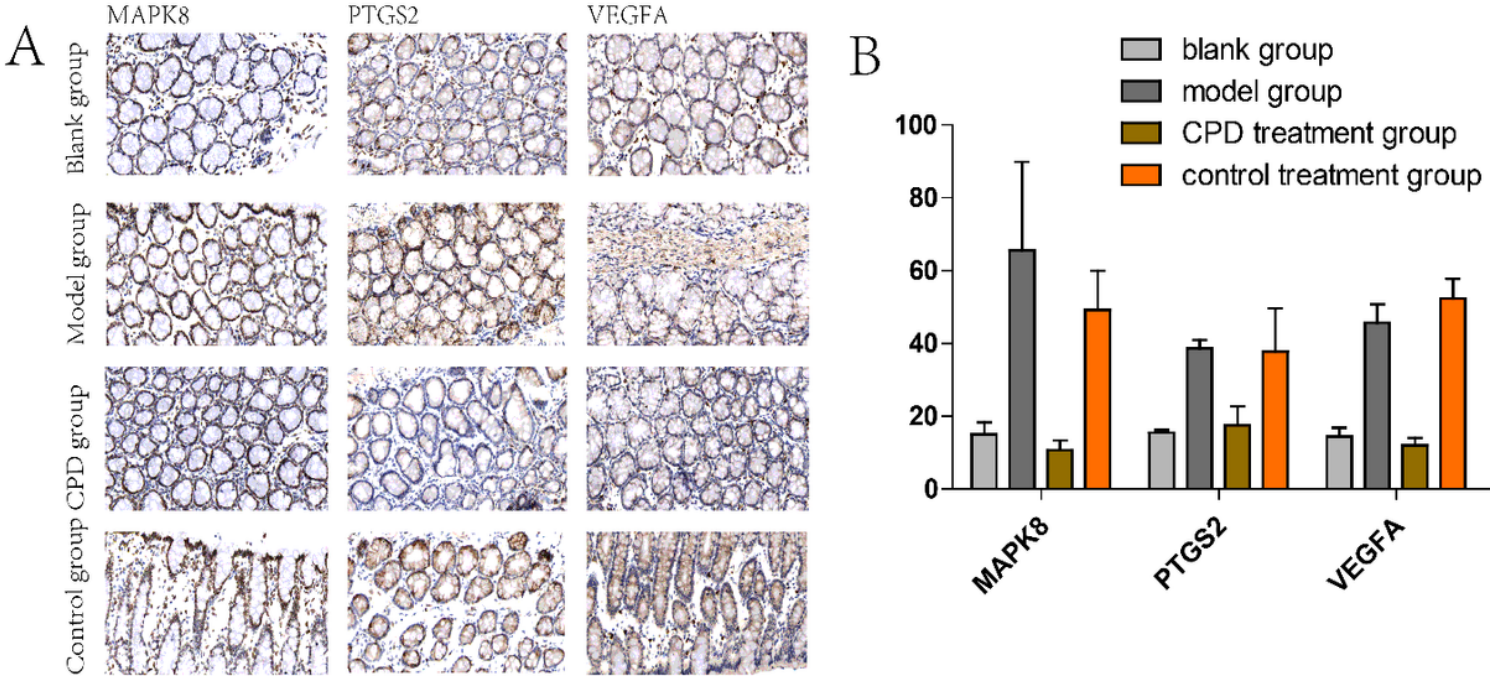

Figure 9

part (A) is result of immunohistochemistry experiments. Part (B) is result of quantitative analysis of immunohistochemistry results. We can find that the expression of MAPK8, PTGS2 and VEGFA of the model group and the control treatment group is higher in proportion to the blank group and CPD treatment group.

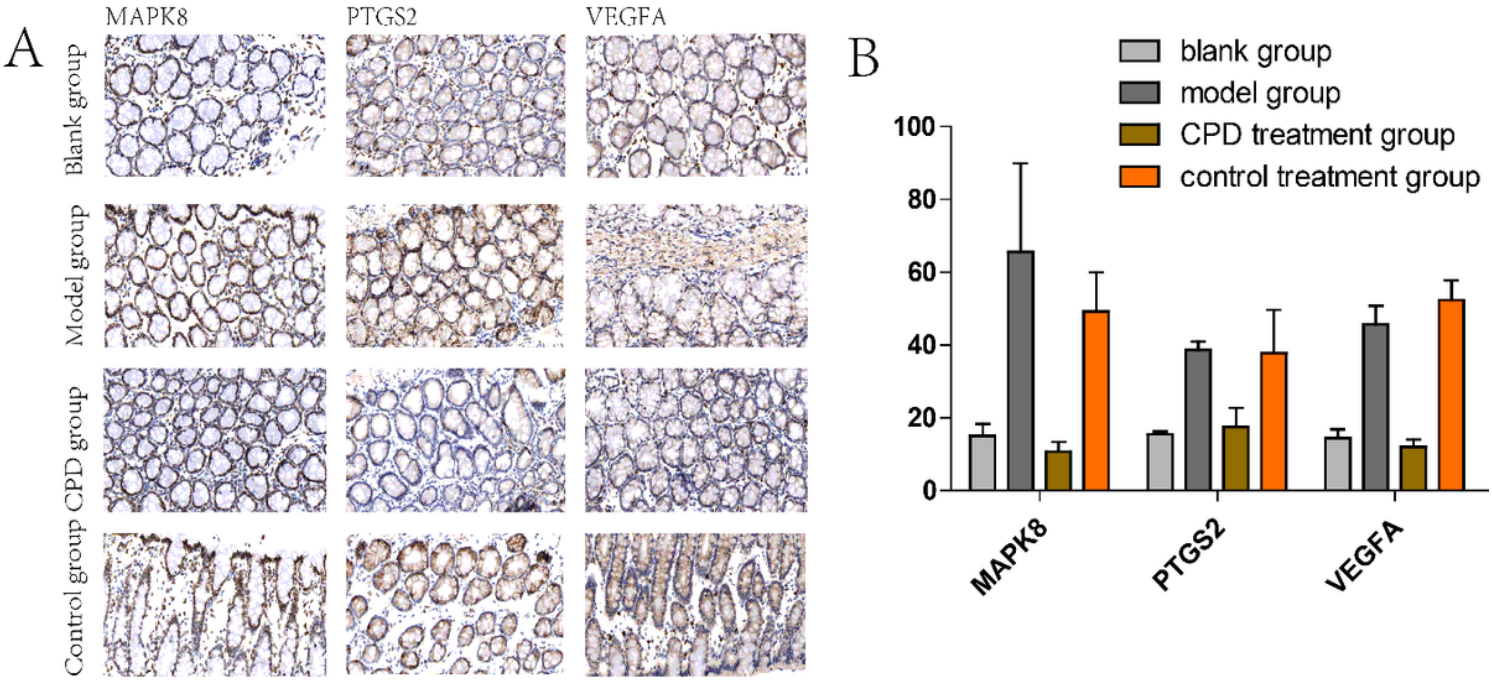

Figure 9

part (A) is result of immunohistochemistry experiments. Part (B) is result of quantitative analysis of immunohistochemistry results. We can find that the expression of MAPK8, PTGS2 and VEGFA of the model group and the control treatment group is higher in proportion to the blank group and CPD treatment group.

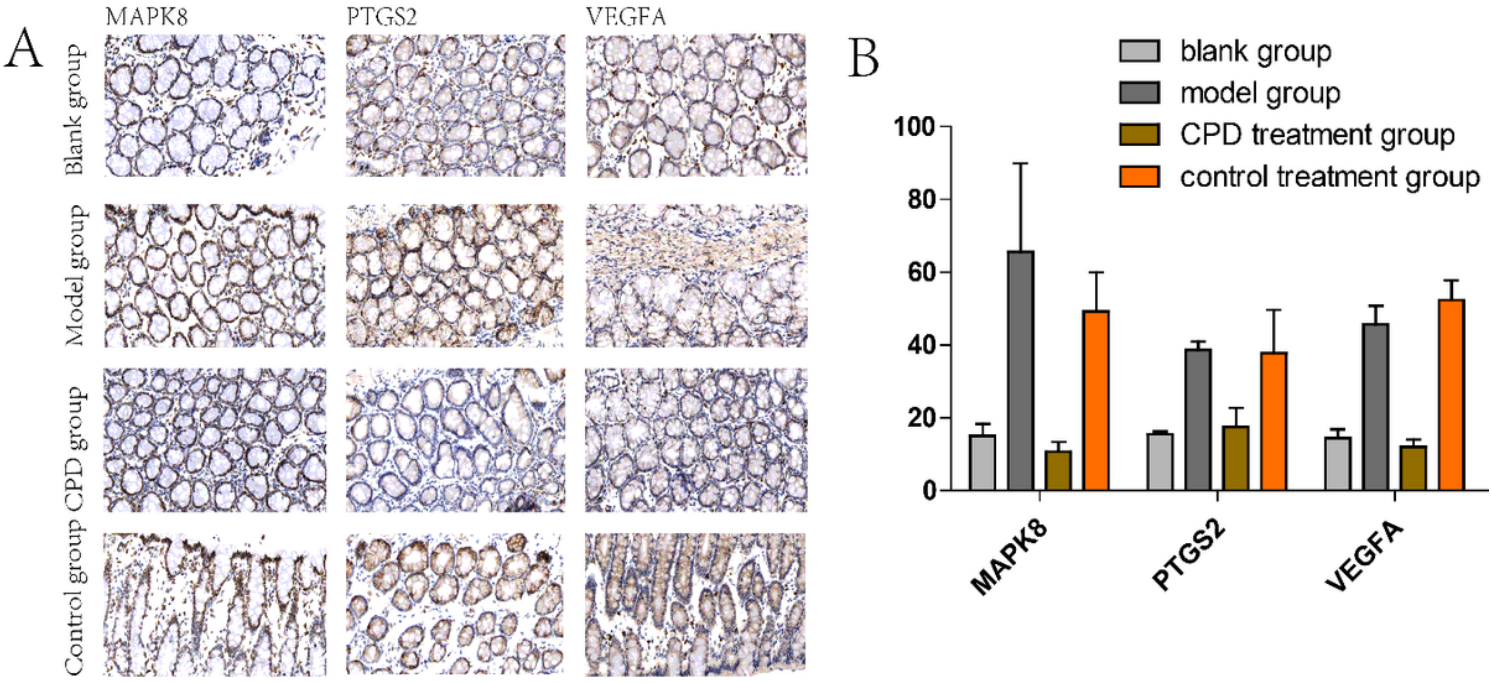

Figure 9

part (A) is result of immunohistochemistry experiments. Part (B) is result of quantitative analysis of immunohistochemistry results. We can find that the expression of MAPK8, PTGS2 and VEGFA of the model group and the control treatment group is higher in proportion to the blank group and CPD treatment group.

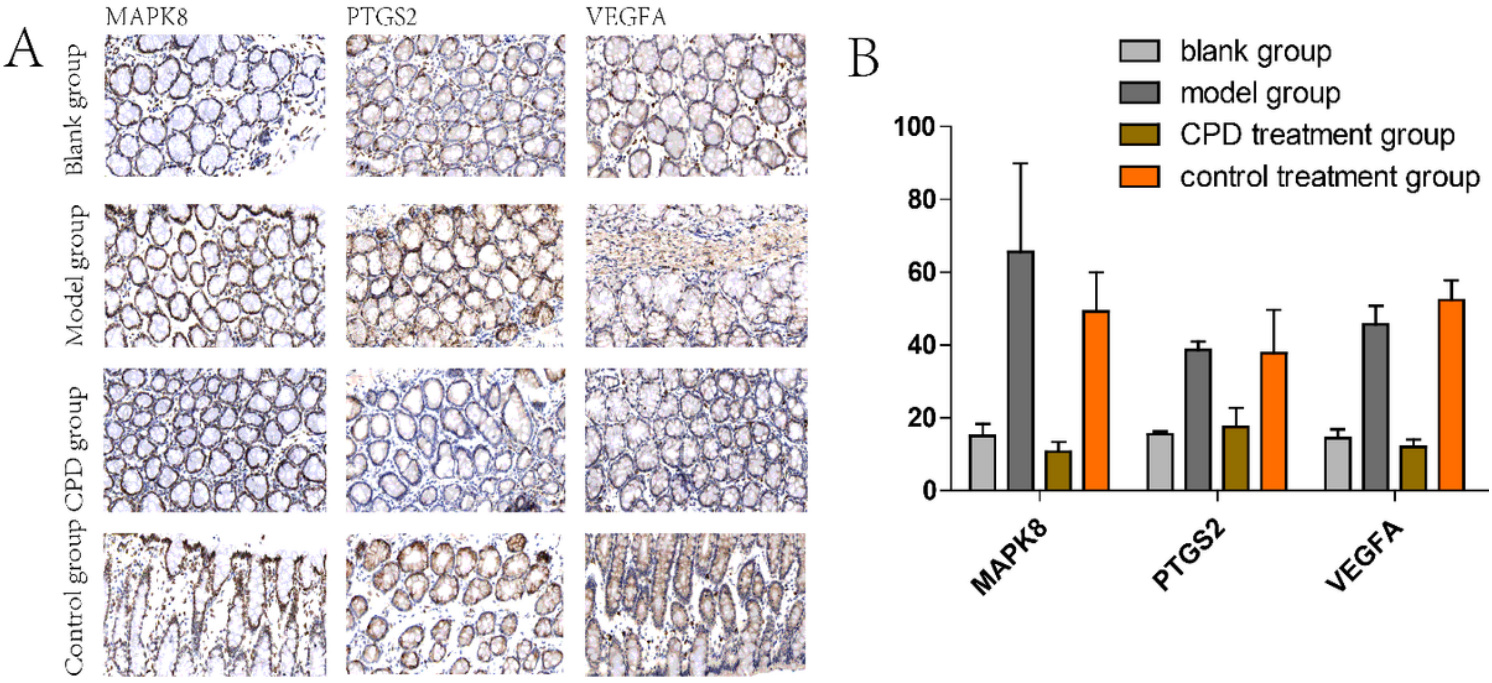

Figure 9

part (A) is result of immunohistochemistry experiments. Part (B) is result of quantitative analysis of immunohistochemistry results. We can find that the expression of MAPK8, PTGS2 and VEGFA of the model group and the control treatment group is higher in proportion to the blank group and CPD treatment group.

Supplementary Files

This is a list of supplementary files associated with this preprint. Click to download.

- arriveguidliensechecklist.docx
- arriveguidliensechecklist.docx
- arriveguidliensechecklist.docx
- arriveguidliensechecklist.docx